

Supporting Information

Manipulation of Intramolecular Hydrogen Bonds in Conjugated Pseudoladder Polymer for Semiconductivity and Solution-Processability

Octavio Miranda¹, Paola Mantegazza², Vikki N. Shinde¹, Zhiqiang Cao³, Steve Shelton⁴, Stefania Moro², Caden Deverter¹, Yi Liu⁴, Xiaodan Gu^{3}, Giovanni Costantini^{2*}, Lei Fang^{1,2*}*

¹ Department of Chemistry, Texas A&M University, 3255 TAMU, College Station, Texas 77843, United States

² School of Chemistry, University of Birmingham, Birmingham B15 2TT, United Kingdom

³ School of Polymer Science and Engineering, The University of Southern Mississippi, Hattiesburg, Mississippi 39406, United States

⁴ The Molecular Foundry, Lawrence Berkeley National Laboratory, One Cyclotron Road, Berkeley, California 94720, United States

Supporting Information

***Corresponding Addresses**

Professor Lei Fang
*Department of Chemistry,
Texas A&M University
3255 TAMU, College Station,
Texas 77843-3255, US
Tel: +1 (979) 845 3186
E-mail: fang@chem.tamu.edu*

Professor Giovanni Costantini
*School of Chemistry,
University of Birmingham
University Rd W, Edgbaston,
Birmingham B15 2TT, UK
Tel: +44 (0121) 414 3155
E-mail: g.costantini@bham.ac.uk*

Professor Xiaodan Gu
*School of Polymer Science &
Engineering, The University of
Southern Mississippi
118 College Drive #5050,
Hattiesburg, Mississippi 39406, US
Tel: +1 (601) 2664868
E-mail: xiaodan.gu@usm.edu*

Table of Content

1. General Information.....	S3
2. Synthesis.....	S4
3. ^1H , ^{13}C NMR.....	S10
4. Fourier Transform Infrared Spectroscopy.....	S22
5. Gel Permeation Chromatography.....	S23
6. Thermal Properties.....	S24
7. Solvent Resistance.....	S25
8. UV-Vis Spectroscopy.....	and Fluorescence Spectroscopy.....S27
9. Cyclic Voltammetry.....	S31
10. Density Functional Theory.....	S32
11. Scanning Tunneling Microscopy.....	S34
12. Transistor Device Fabrication and Measurement.....	S36

13. Atomic

Force

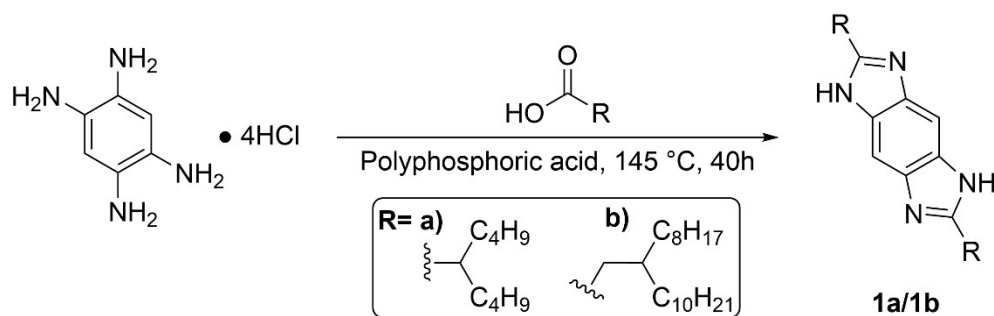
Microscopy.....S39

14. References.....S40

1. General Information

Starting materials and reagents were purchased from AstaTech, BLD Pharm, TCI Chemicals, Oakwood, or Combi-Blocks and were used without further purification unless otherwise specified. THF was dried and distilled under nitrogen from sodium using benzophenone as the indicator. Toluene was dried and purified using an Innovative Technology pure solvent system (PureSolv-MD-5). 1,2,4,5-tetraminobenzene hydrochloric acid^{S1} and benzofuran-2-yltrimethylstannane^{S2} were synthesized according to reported literature procedures. Compound (4,8-Bis(5-(2-ethylhexyl)thiophen-2-yl)benzo[1,2-b:4,5-b']difuran-2,6-diyl)bis(trimethylstannane) was purchased from BLD Pharm. Preparative gel permeation chromatography (GPC) was performed in chloroform solution at room temperature with an eluting rate of 14 mL/min using Japan Analytical Industry recycling preparative HPLC (LC-92XXII NEXT SERIES). ¹H and ¹³C NMR spectra were recorded on a Varian Inova 400 MHz spectrometer or a Varian VnmrS 500 MHz spectrometer. The NMR chemical shifts were reported in ppm relative to the signals corresponding to the residual non-deuterated solvents (CDCl₃: ¹H 7.26 ppm, ¹³C 77.16 ppm) or the internal standard (tetramethylsilane: ¹H 0.00 ppm). Abbreviations for reported signal multiplicities are as follows: s, singlet; d, doublet; t, triplet; q, quartet; m, multiplet; br, broad. High resolution mass spectra were obtained via electrospray ionization (ESI) on an Applied Biosystems PE SCIEX QSTAR with a time-of-flight (TOF) analyzer. Automatic flash column chromatography was carried out using Biotage® Isolera™ Prime instrument with various size of SiO₂ Biotage ZIP® cartridge. Gel Permeation Chromatography (GPC) was performed on TOSOH EcoSEC (HLC-8320GPC) in THF solution at 40°C temperature and the molecular weights calculated using a calibration curve based on polystyrene standards, equipped with TSKgel SuperHM-M and TSKgel SuperH-RC. Fourier transform infrared (FTIR) Spectroscopy was recorded by attenuated total reflectance using a Shimadzu IRAffinity-1S spectrometer with a KBr crystal. UV-vis absorption spectra were recorded on a Shimadzu UV-2600 Spectrophotometer. Fluorescence spectra were recorded on the Horiba Scientific FluoroMax®-4.

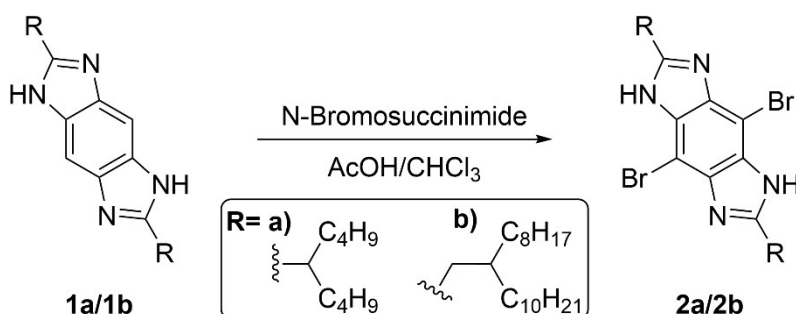
2. Synthesis



2,6-Di(nonan-5-yl)-1,5-dihydrobenzo[1,2-d:4,5-d']diimidazole (1a). To a 100 mL round bottom flask with a magnetic stirring bar was added 1,2,4,5-tetraaminobenzene hydrochloric acid (1.08 g, 3.81 mmol), 2-butylhexanoic acid (1.64 g, 5.53 mmol), and polyphosphoric acid (9 g). The flask was fitted with a condenser and flushed with nitrogen before being heated initially to 100 °C for 1 h, The mixture was subsequently heated to 140 °C and allowed to stir under nitrogen atmosphere for 40 h. The viscous mixture was poured over ice water (~100 mL) with vigorous stirring and then basified by the addition of NaOH pellets. The solid suspension was allowed to stir until it became a well dispersed powder and no large clumps remained, then filtered through a glass frit and washed well with DI water and cold acetone. The powder was collected and dried under vacuum to afford **1a** (1.49 g, 98%) as a tan solid, which was used in the next step without further purification. ¹H NMR (400 MHz, CDCl₃ + trifluoroacetic acid-D₁): δ 12.72 (br, 4H), 8.37 (s, 2H), 3.30 (m, 2H), 1.96 (m, 4H), 1.86 (m, 4H), 1.31 (m, 12H), 1.15 (m, 4H), 0.85 (t, *J* = 7.0 Hz, 12H). ¹³C NMR (100 MHz, CDCl₃ + trifluoroacetic acid-*d*₁): δ 161.76, 129.42, 100.04, 39.96, 33.49, 29.32, 22.25, 13.46. HRMS *m/z*: (ESI-TOF): [*M* + *H*]⁺ Calc'd for C₂₆H₄₂N₄ 411.3482; Found 411.3476.

2,6-Bis(2-octyldodecyl)-1,5-dihydrobenzo[1,2-d:4,5-d']diimidazole (1b). 1,2,4,5-tetraaminobenzene hydrochloric acid (1.36 g, 4.79 mmol), 3-octyltridecanoic acid (3.80 g, 10.5 mmol), and polyphosphoric acid (10 g) combined using the same procedure as for **1a**. **1b** was obtained as a tan solid, which was used in the next step without further purification (3.34 g, 97%). ¹H NMR (400 MHz, CDCl₃ + trifluoroacetic acid-*d*₁): δ 8.37 (s, 2H), 3.17 (d, *J* = 7.3 Hz, 4H), 2.05 (br, 2H) 1.42 (br, 4H), 1.25 (br, 60H), 0.86 (m, 12H, *J* = 6.2 Hz). ¹³C NMR (100 MHz, CDCl₃ + trifluoroacetic acid-D₁): δ 157.83, 129.40, 99.80, 38.50, 33.49, 32.40, 32.05, 31.95, 29.77, 29.71,

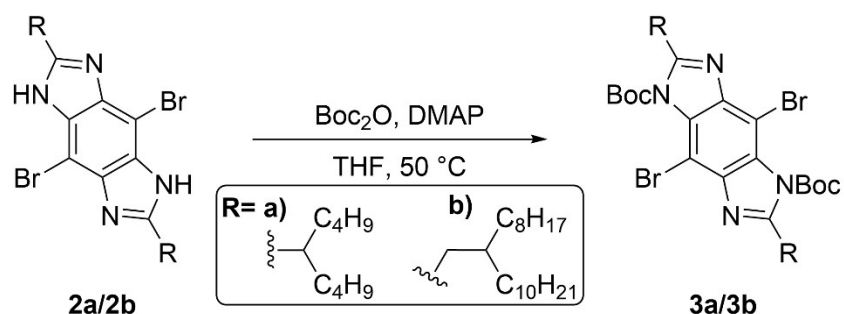
29.69, 29.59, 29.52, 29.46, 29.32, 26.25, 22.81, 22.74, 14.08, 14.02. HRMS m/z : (ESI-TOF): $[M + H]^+$ Calc'd for $C_{48}H_{86}N_4$ 719.6931; Found 719.6908.



4,8-Dibromo-2,6-di(nonan-5-yl)-1,5-dihydrobenzo[1,2-d:4,5-d']diimidazole (2a). In a 100 mL round bottom with a magnetic stirring bar, compound **1a** (1.05 g, 2.56 mmol) was dissolved in a mixed solvent (30 mL) of acetic acid (10% v/v) and chloroform (90% v/v). To this solution was added *N*-bromosuccinimide (1.14 g, 6.40 mmol) in one portion. Precipitate formed in the reaction flask within 10 minutes of addition, after which the reaction mixture was allowed to stir for an additional 30 minutes before solvent was removed via rotary evaporator. Acetone was added to break down residue on the sides of the round bottom flask, and saturated sodium bicarbonate (aq) was used to neutralize any remaining acetic acid. The suspension in acetone/ $NaCO_3$ (aq) was filtered through a glass frit and washed with water and cold acetone before being collected and dried under high vacuum to give product **2a** as an off-white powder (1.25 g, 85%). **2a** was used in the next step without further purification. 1H NMR (400 MHz, $CDCl_3$ + trifluoroacetic acid- D_1): 3.35 (br, 2H), 1.96 (m, 8H), 1.32 (br, 12H), 1.12 (br, 4H), 0.84 (t, $J = 6.3$ Hz, 12H). ^{13}C NMR (100 MHz, $CDCl_3$ + trifluoroacetic acid- d_1): δ 164.21, 129.95, 90.54, 40.99, 33.82, 29.75, 22.32, 13.20. HRMS m/z : (ESI-TOF): $[M + H]^+$ Calc'd for $C_{26}H_{40}Br_2N_4$ 567.1692; Found 567.1683.

4,8-Dibromo-2,6-bis(2-octyldodecyl)-1,5-dihydrobenzo[1,2-d:4,5-d']diimidazole (2b). Compound **1b** (1.17 g, 1.63 mmol), *N*-bromosuccinimide (0.64 g, 3.1 mmol), and mixed solvent (30 mL) were combined using the same procedure as for **2a**. Precipitate was not observed in this case. **2b** was obtained as a off-white solid, which was used in the next step without further purification (1.23 g, 86%). 1H NMR (400 MHz, $CDCl_3$ + trifluoroacetic acid- d_1): δ 3.18 (d, $J = 7.1$ 4H), 2.09 (br, 2H), 1.42 (br, 4H), 1.23 (br, 60H), 0.86 (m, 12H, $J = 5.7$ Hz). ^{13}C NMR (100 MHz, $CDCl_3$ + trifluoroacetic acid- D_1): δ 160.46, 129.97, 90.11, 39.12, 33.55, 32.69, 32.06, 31.95,

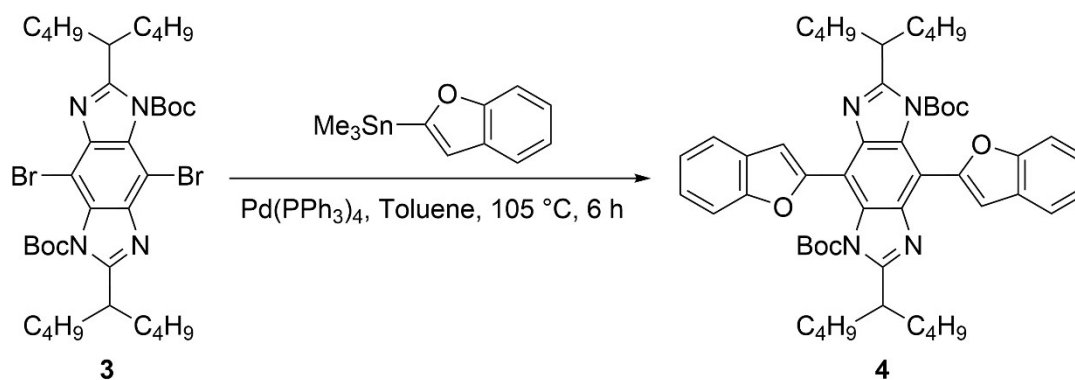
29.77, 29.72, 29.61, 29.54, 29.46, 29.33, 26.27, 22.80, 22.74, 14.03, 13.96. HRMS m/z : (ESI-TOF): $[M + H]^+$ Calc'd for $C_{48}H_{84}Br_2N_4$ 875.5136; Found 875.5109.



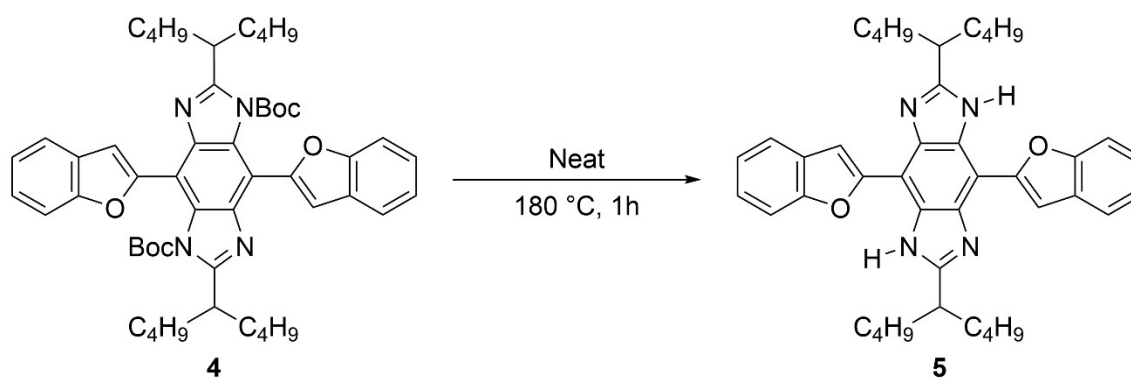
Di-tert-butyl-4,8-dibromo-2,6-di(nonan-5-yl)benzo[1,2-d:4,5-d']diimidazole-1,5-dicarboxylate (3a). To a 250 mL round bottom with a magnetic stirring bar, compound **2a** (1.09 g, 1.92 mmol) and 4-dimethylaminopyridine (0.47 g, 3.9 mmol) were added together with anhydrous THF (40 mL). To this stirring suspension was added di-tert-butyl dicarbonate (1.05 g, 4.82 mmol) dissolved in anhydrous THF (20 mL). The temperature was elevated to 50 °C and the reaction mixture was allowed to stir for an hour. As the reaction progressed, the suspension dissolved to become a homogenous solution. After removing solvent, the residue was subjected to silica gel flash column chromatography (SiO_2 ; hexanes/ CH_2Cl_2 1:1) to afford **3a** as a white solid (0.81 g, 55%). ^1H NMR (400 MHz, CDCl_3): δ 3.22 (m, 2H), 1.98 (m, 4H), 1.76 (m, 4H), 1.70 (s, 18H), 1.27 (m, 12H), 1.19 (m, 4H), 0.84 (t, $J = 7.0$ Hz, 12H). ^{13}C NMR (100 MHz, CDCl_3): δ 160.89, 148.61, 140.82, 129.64, 94.69, 87.01, 39.17, 34.67, 30.04, 27.93, 22.84, 14.12. HRMS m/z : (ESI-TOF): $[M + H]^+$ Calc'd for $C_{36}H_{56}Br_2N_4O_4$ 767.2741; Found 767.2714.

Di-tert-butyl-4,8-dibromo-2,6-bis(2-octyldodecyl)benzo[1,2-d:4,5-d']diimidazole-1,5-dicarboxylate (3b). Compound **2a** (1.09 g, 1.92 mmol), 4-dimethylaminopyridine (0.47 g, 3.4 mmol), di-tert-butyl dicarbonate (0.93 g, 4.3 mmol), and THF (36 and 18 mL) were combined using the same procedure as for **3a**. After removing solvent, the residue was subjected to silica gel flash column chromatography (SiO_2 ; hexanes/ CH_2Cl_2 4:1) to afford **3b** as a clear oil (0.94 g, 51%). ^1H NMR (400 MHz, CDCl_3): δ 3.00 (d, $J = 7.4$, 4H), 2.07 (br, 2H), 1.69 (s, 18H), 1.34 (br, 8H), 1.23 (br, 56H), 0.86 (m, $J = 6.9$ Hz, 12H). ^{13}C NMR (100 MHz, CDCl_3 + trifluoroacetic acid- D_1): δ 157.09, 148.33, 140.88, 129.96, 95.05, 86.98, 37.26, 34.50, 33.56, 32.07, 32.05, 32.02, 30.06, 29.85, 29.80, 29.77, 29.74, 29.68, 29.51, 29.48, 29.42, 27.92, 26.42, 22.82, 22.79, 14.55, 14.25,

14.23. HRMS m/z : (ESI-TOF): $[M + H]^+$ Calc'd for $C_{58}H_{100}Br_2N_4O_4$ 1075.6184; Found 1075.6103.

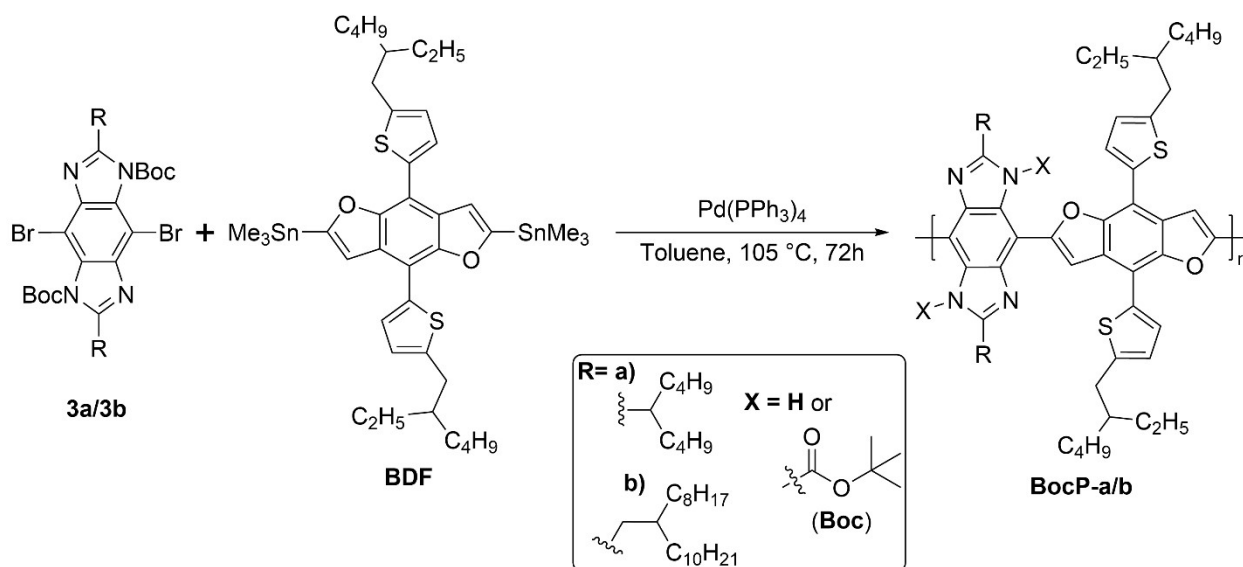


Di-tert-butyl 4,8-di(benzofuran-2-yl)-2,6-di(nonan-5-yl)benzo[1,2-d:4,5-d']diimidazole-1,5-dicarboxylate (4). To an anhydrous and degassed solution of compound **3a** (400 mg, 0.520 mmol) and benzofuran-2-yltrimethylstannane (439 mg, 1.56 mmol) in toluene (12 mL) was added tetrakis(triphenylphosphine)palladium(0) (60 mg, 0.052 mmol, 10 mol%) under the flow of nitrogen. The solution was heated to 105 °C and allowed to stir for 6 h. After removing solvent, the residue was subjected to flash column chromatography (SiO_2 ; hexanes/ CH_2Cl_2 2:1) to afford **4** as a pale yellow solid (309 mg, 73%). 1H NMR (400 MHz, $CDCl_3$): δ 7.94 (s, 2H), 7.73 (m, 2H), 7.50 (m, 2H), 7.27 (m, 4H), 3.64 (p, $J = 6.7$ Hz, 2H), 2.08 (m, 4H), 1.81 (m, 4H), 1.38 (m, 16H), 1.18 (s, 18H), 0.90 (t, $J = 6.9$ Hz, 12H). ^{13}C NMR (100 MHz, $CDCl_3$): δ 162.00, 154.45, 151.55, 149.49, 139.66, 129.52, 128.22, 124.22, 122.98, 121.53, 111.78, 108.59, 108.27, 85.39, 38.83, 34.56, 29.87, 27.70, 23.02, 14.19. FTIR (neat) cm^{-1} : 2951 (m), 2926 (m), 2861 (m), 1757 (s), 1122 (s). HRMS m/z : (ESI-TOF): $[M + H]^+$ Calc'd for $C_{52}H_{66}N_4O_6$ 843.5055; Found 843.5051.



4,8-Di(benzofuran-2-yl)-2,6-di(nonan-5-yl)-1,5-dihydrobenzo[1,2-d:4,5-d']diimidazole (5).

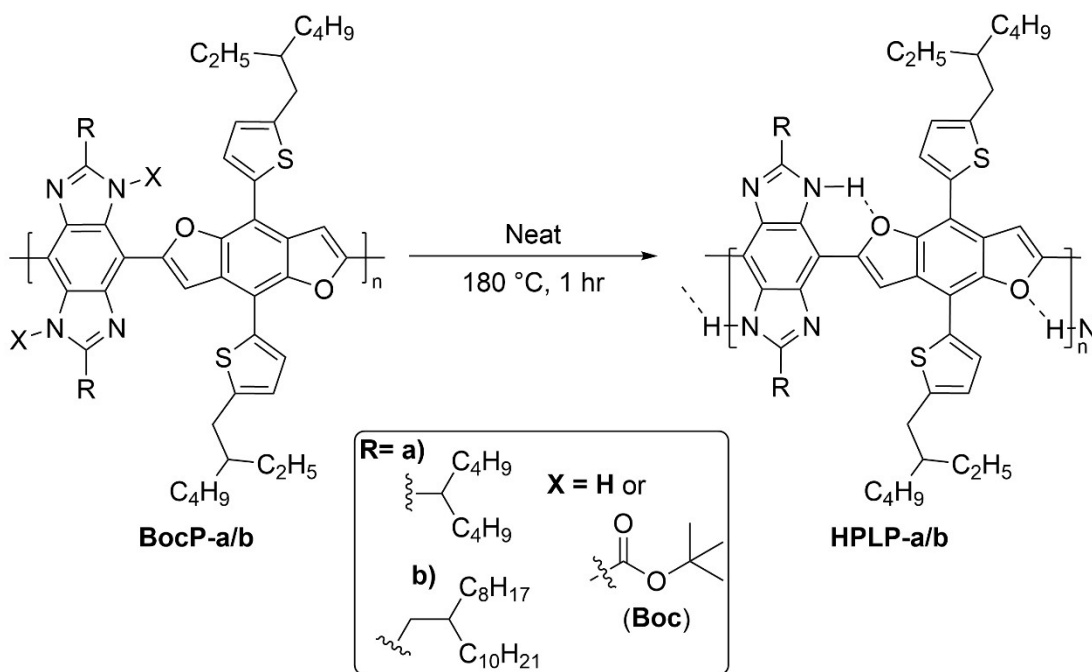
Compound **4** (152 mg, 0.180 mmol) was transferred to a 20 mL vial and attached to a Schlenk line where it was evacuated and refilled with nitrogen 3 times to create an inert atmosphere. The vial was heated to 180 °C for 1 h and subsequently allowed to cool to room temperature to yield **5** (116 mg, quantitative) as a bright yellow solid. No purification was needed. ¹H NMR (400 MHz, CDCl₃): δ 10.16 (s, 2H), 8.35 (s, 2H), 7.75 (d, *J* = 6.9 Hz, 2H), 7.65 (d, *J* = 7.8 Hz, 2H), 7.34 (m, 4H), 3.15 (br, 2H), 1.95 (m, 8H), 1.40 (m, 16H), 0.92 (t, *J* = 7.0 Hz, 12H). ¹³C NMR (100 MHz, CDCl₃): δ 159.38, 154.21, 153.08, 137.38, 129.75, 127.58, 124.28, 123.42, 121.71, 110.75, 107.74, 103.19, 40.88, 34.63, 29.90, 22.94, 14.15. FTIR (neat) cm⁻¹: 3450 (m), 2955 (m), 2927 (m), 2853 (m), 1320 (s). HRMS *m/z*: (ESI-TOF): [M + H]⁺ Calc'd for C₄₂H₅₀N₄O₂ 643.4007; Found 643.3984.



BocP-a. To a 100 mL schlenk tube was added compound **3a** (201 mg, 0.261 mmol), 4,8-Bis(5-(2-ethylhexyl)thiophen-2-yl)benzo[1,2-b:4,5-b']difuran-2,6-diylbis(trimethylstannane) (**BDF**) (228 mg, 0.261 mmol), and Pd(PPh₃)₄ (15 mg, 0.013 mmol, 5 mol%) under nitrogen atmosphere and sealed by a rubber septum. Anhydrous toluene (15 mL) was added to the reaction mixture via needle and syringe. The reaction mixture was degassed by freeze-pump-thaw method. The resulting solution was heated to 105 °C and allowed to stir for 72 h. After evaporating solvent, the residue was redissolved in minimal chloroform and precipitated by adding it dropwise to a cold methanol solution under vigorous stirring. The crude dark orange powder was purified by

preparative GPC and separated in 3 fractions shown in **Table S1** (277 mg, 92%). $^1\text{H NMR}$ (400 MHz, CDCl_3): δ 10.67 (br, 0.3H), 9.04 (br, 1.5H), 7.94 (br, 2.4H), 7.01 (br, 2.0H), 3.77 (br, 1.3H), 2.98 (br, 4.2H), 2.03 (br, 8.7H), 1.42 (br, 31H), 1.14 (br, 10.8H), 0.94 (br, 23.1H). FTIR (neat) cm^{-1} : 3417 (w), 2954 (m), 2925 (m), 2857 (m), 1750 (s), 1126 (s). GPC (THF, 40 °C) $M_n = 11.5$ kg/mol, $D = 2.15$.

BocP-b. Compound **3b** (184 mg, 0.171 mmol), BDF (149 mg, 0.171 mmol), and $\text{Pd}(\text{PPh}_3)_4$ (10 mg, 0.0085 mmol, 5 mol%) were combined using the same as procedure as **BocP-a**. The crude dark orange powder was purified by preparative GPC to remove low molecular weight oligomers. Further removal of chloroform under reduced pressure afforded **BocP-b** as a dark orange film (183 mg, 83%). $^1\text{H NMR}$ (400 MHz, CDCl_3): δ 10.76 (br, 0.1H), 8.66 (br, 0.9H), 7.90 (br, 2.1H), 6.90 (br, 2.0H), 3.23 (br, 1.7H), 2.96 (br, 4.0H), 2.46 (br, 1.1H), 1.97 (br, 0.8H), 1.10 (br, 110.9H). FTIR (neat) cm^{-1} : 3415 (w), 2955 (m), 2921(m), 2852 (m), 1752 (s), 1132 (s). GPC (THF, 40 °C) $M_n = 28.6$ kg/mol, $D = 1.98$.



HPLP-a. Polymer **BocP-a** was transferred to a 20 mL vial and attached to a schlenk line via adapter where it was evacuated and refilled with nitrogen 3 times to create an inert atmosphere. The solid was heated in the vial to 180 °C for 1 hour and then was allowed to cool to room temperature to yield **HPLP-a**. No purification was performed. (quantitative). $^1\text{H NMR}$ (400 MHz,

CDCl₃): δ 10.69 (br, 2H), 9.02 (br, 2H), 7.87 (br, 2H), 7.13 (br, 2H), 3.12 (br, 6H), 2.05 (br, 16H), 1.44 (br, 64H), 0.99 (br, 24H). FTIR (neat) cm⁻¹: 3450 (m), 2955 (m), 2924 (m), 2856 (m), 1757 (s), 1122 (s).

HPLP-b. Same as procedure for **HPLP-a.** ¹H NMR (400 MHz, CDCl₃): δ 10.81 (br, 0.2H), 9.78 (br, 0.7H), 7.77 (br, 2.0H), 7.00 (br, 2.0H), 3.02 (br, 6.0H), 2.33 (br, 1.9H), 1.44 (br, 140.8H). FTIR (neat) cm⁻¹: 3416 (w), 2955 (m), 2921(m), 2851 (m), 1303 (s).

3. ^1H , ^{13}C NMR Spectra

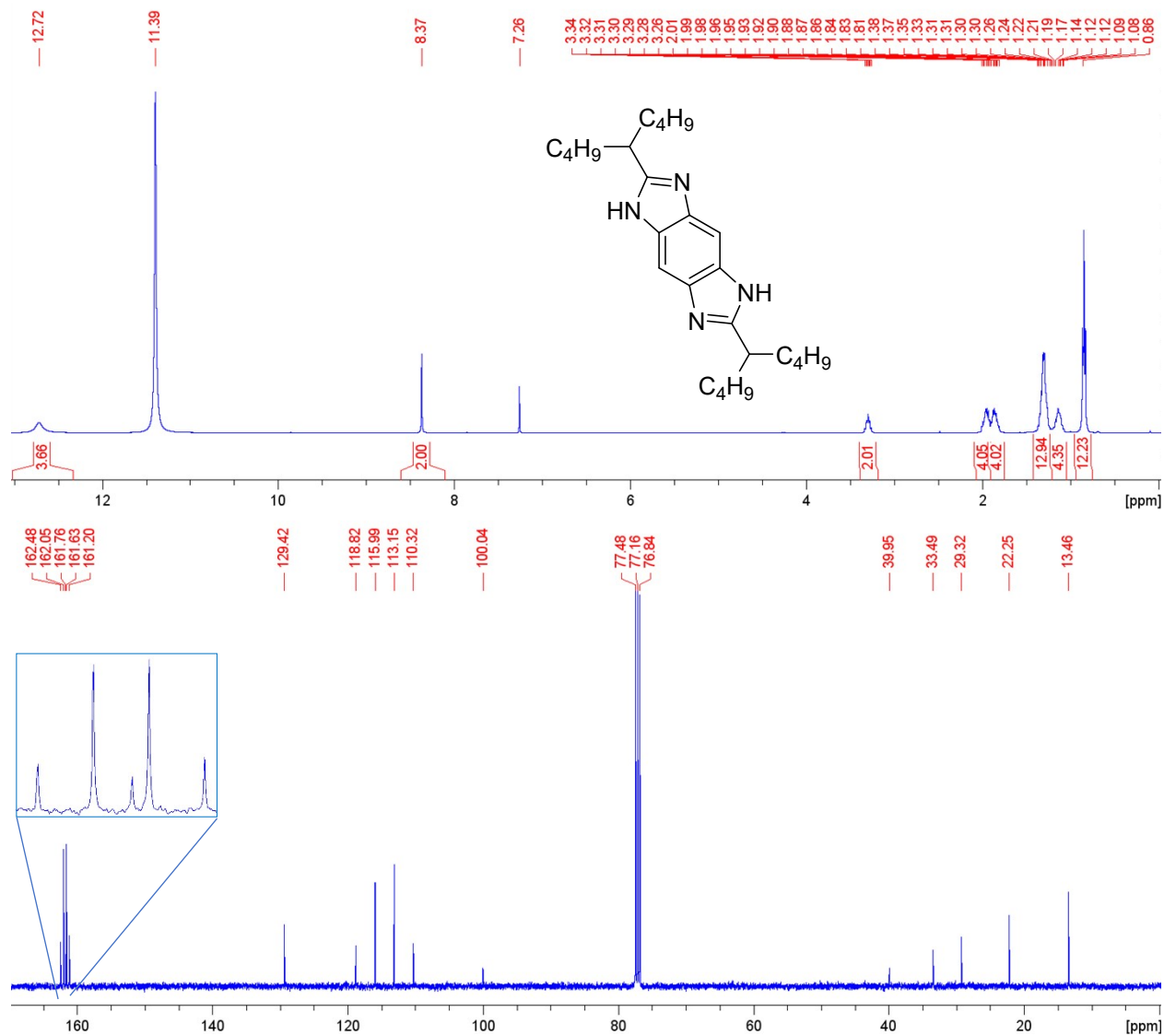


Figure S1. ^1H (400 MHz) and $^{13}\text{C}\{^1\text{H}\}$ (100 MHz) NMR spectra of **1a** at room temperature in a mixed solvent of CDCl_3 and trifluoroacetic acid- d_1 .

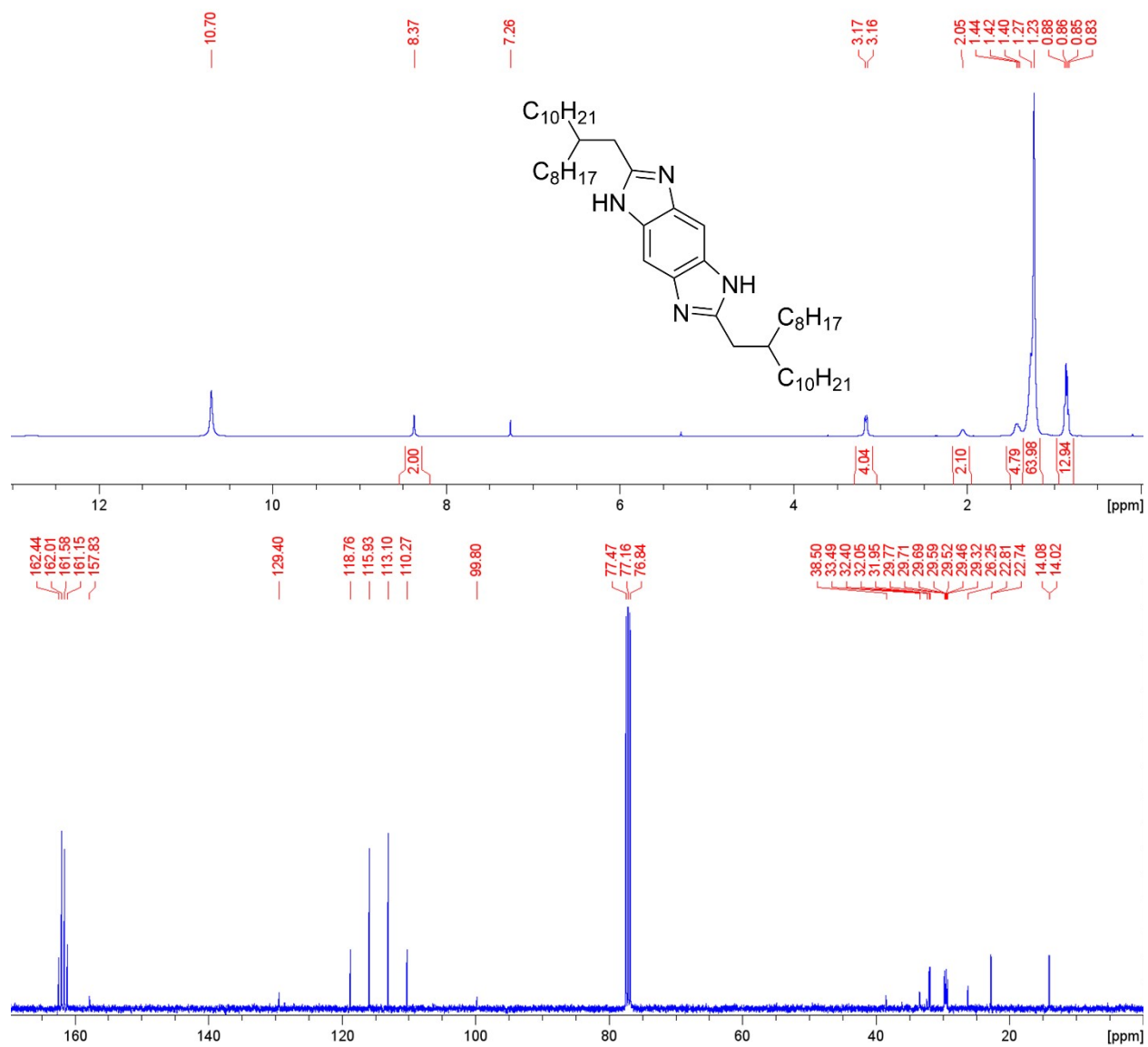


Figure S2. ¹H (400 MHz) and ¹³C{¹H} (100 MHz) NMR spectra of **1b** at room temperature in a mixed solvent of CDCl₃ and trifluoroacetic acid-*d*₁.

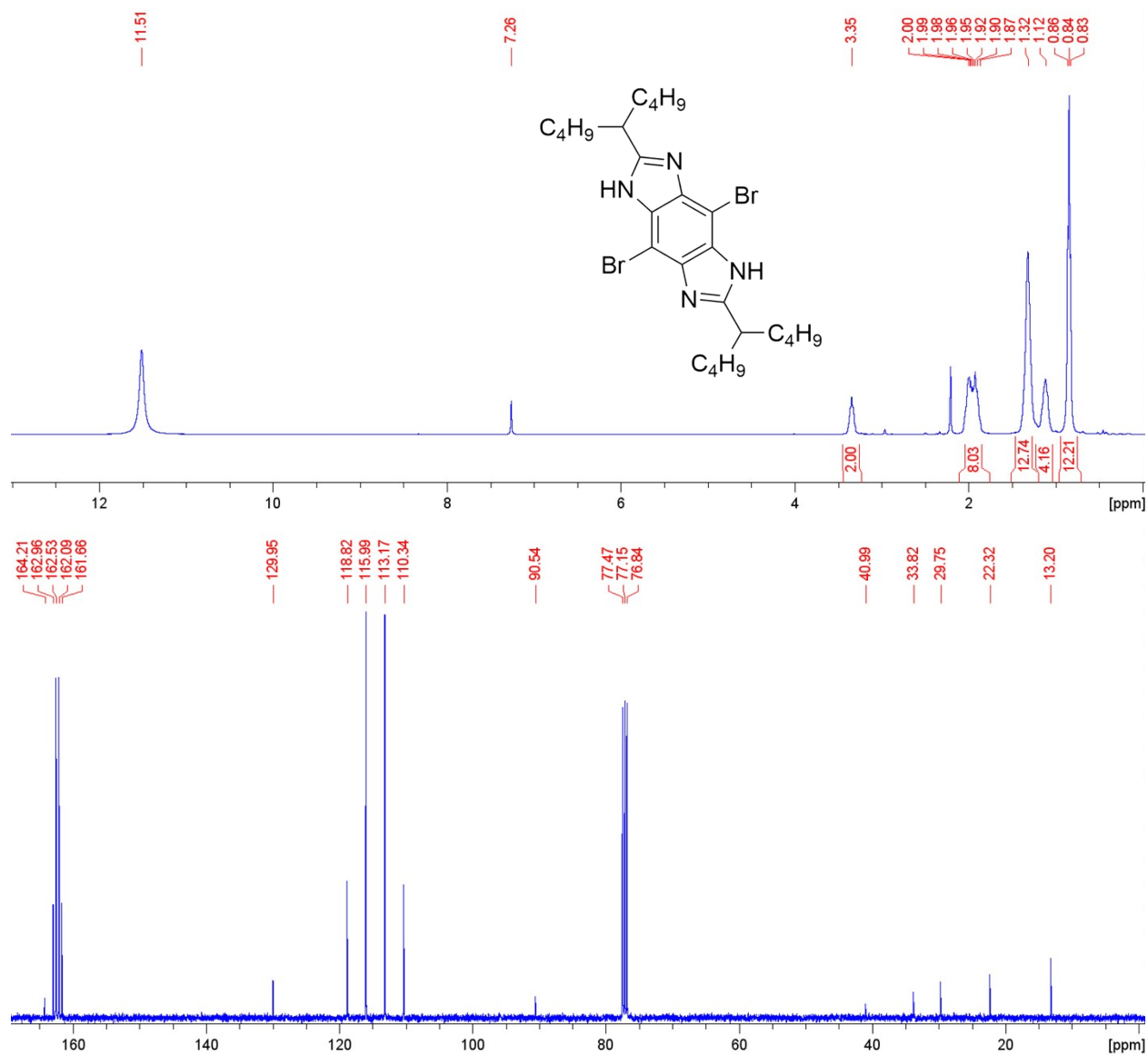


Figure S3. ^1H (400 MHz) and $^{13}\text{C}\{^1\text{H}\}$ (100 MHz) NMR spectra of **2a** at room temperature in a mixed solvent of CDCl_3 and trifluoroacetic acid- d_1 .

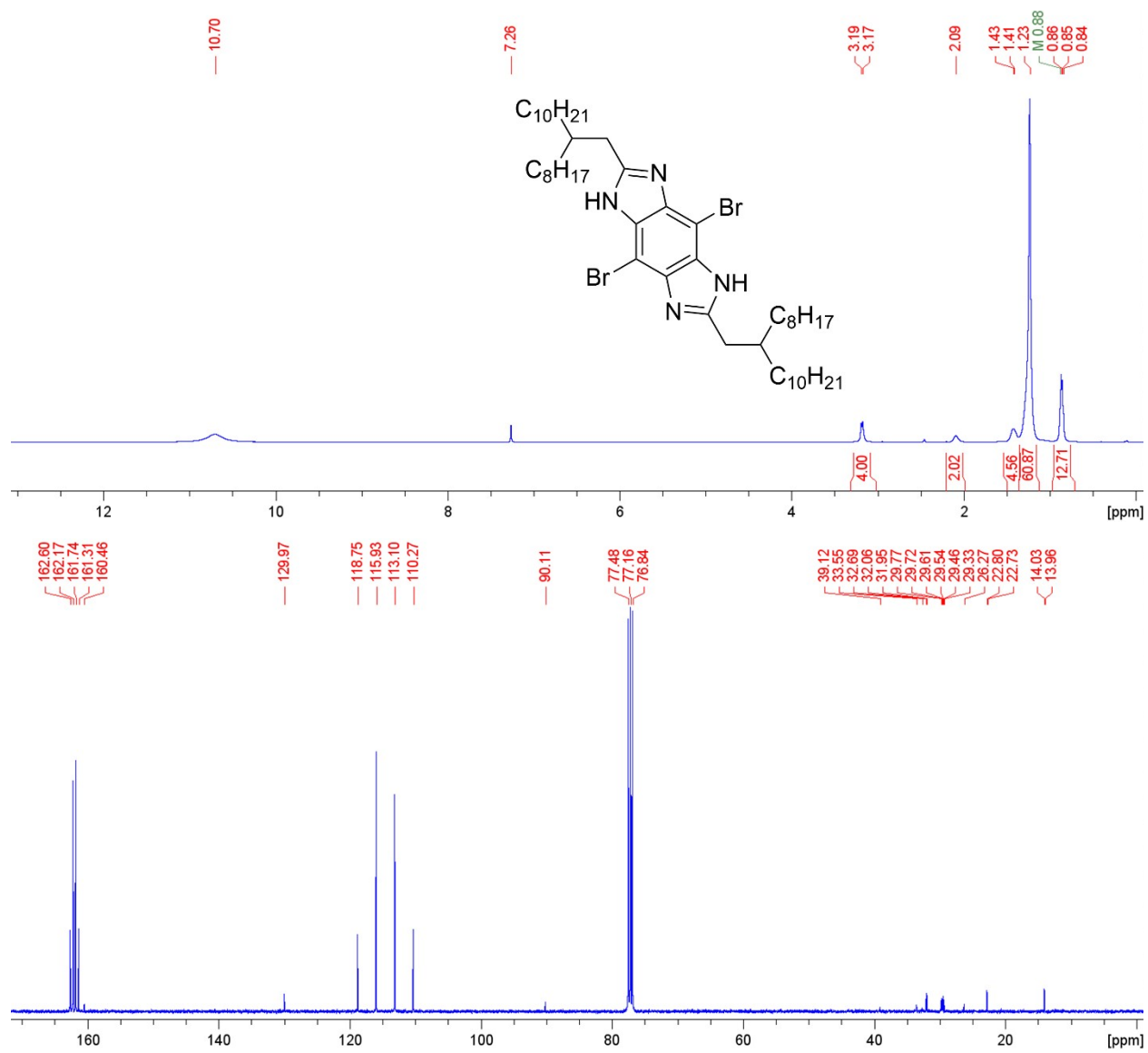


Figure S4. ¹H (400 MHz) and ¹³C{¹H} (100 MHz) NMR spectra of **2b** at room temperature in a mixed solvent of CDCl₃ and trifluoroacetic acid-*d*₁.

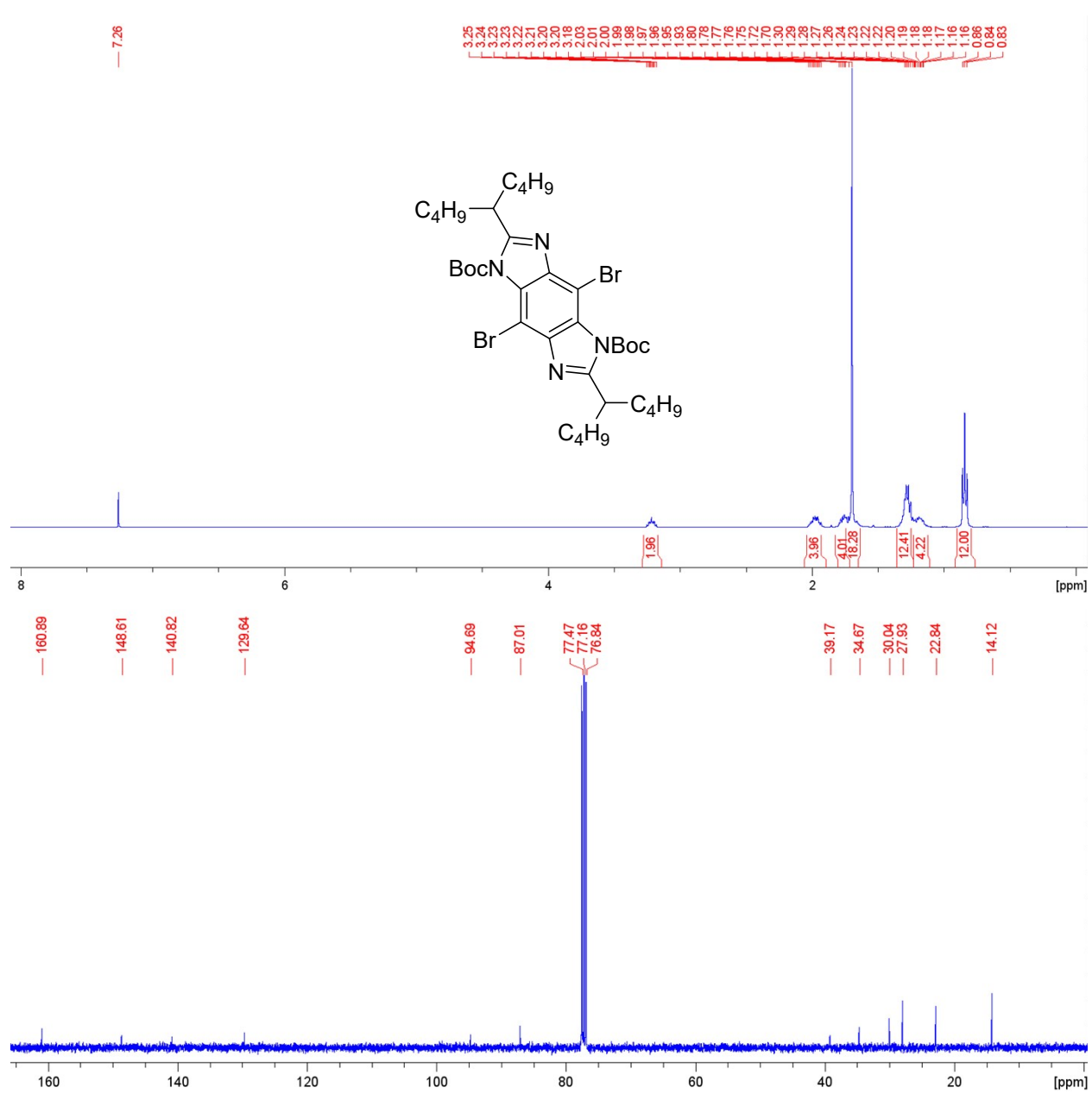


Figure S5. ¹H (400 MHz) and ¹³C{¹H} (100 MHz) NMR spectra of **3a** at room temperature in CDCl₃.

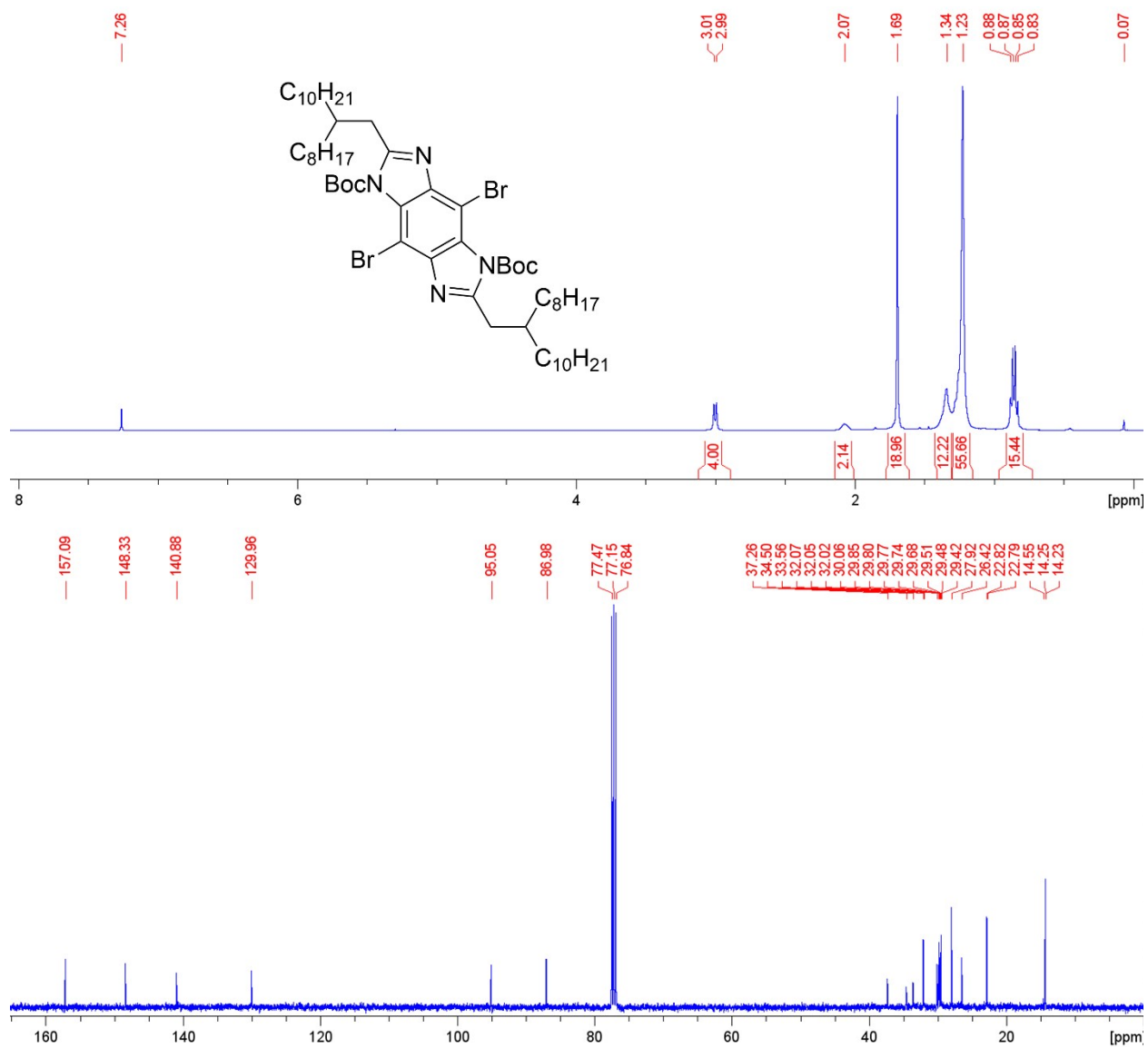


Figure S6. ^1H (400 MHz) and $^{13}\text{C}\{^1\text{H}\}$ (100 MHz) NMR spectra of **3b** at room temperature in CDCl_3 .

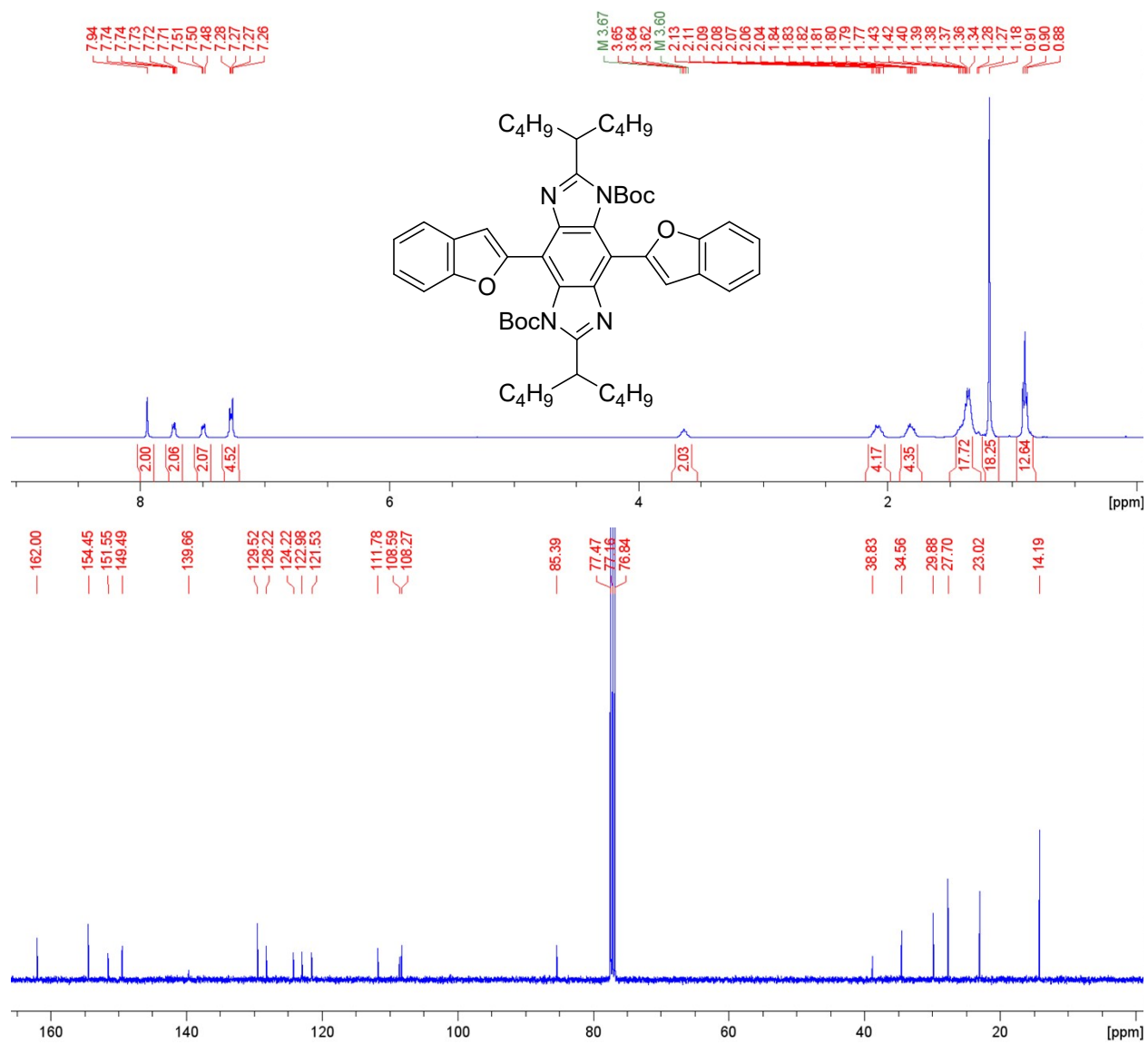


Figure S7. ^1H (400 MHz) and $^{13}\text{C}\{^1\text{H}\}$ (100 MHz) NMR spectra of **4** at room temperature in CDCl_3 .

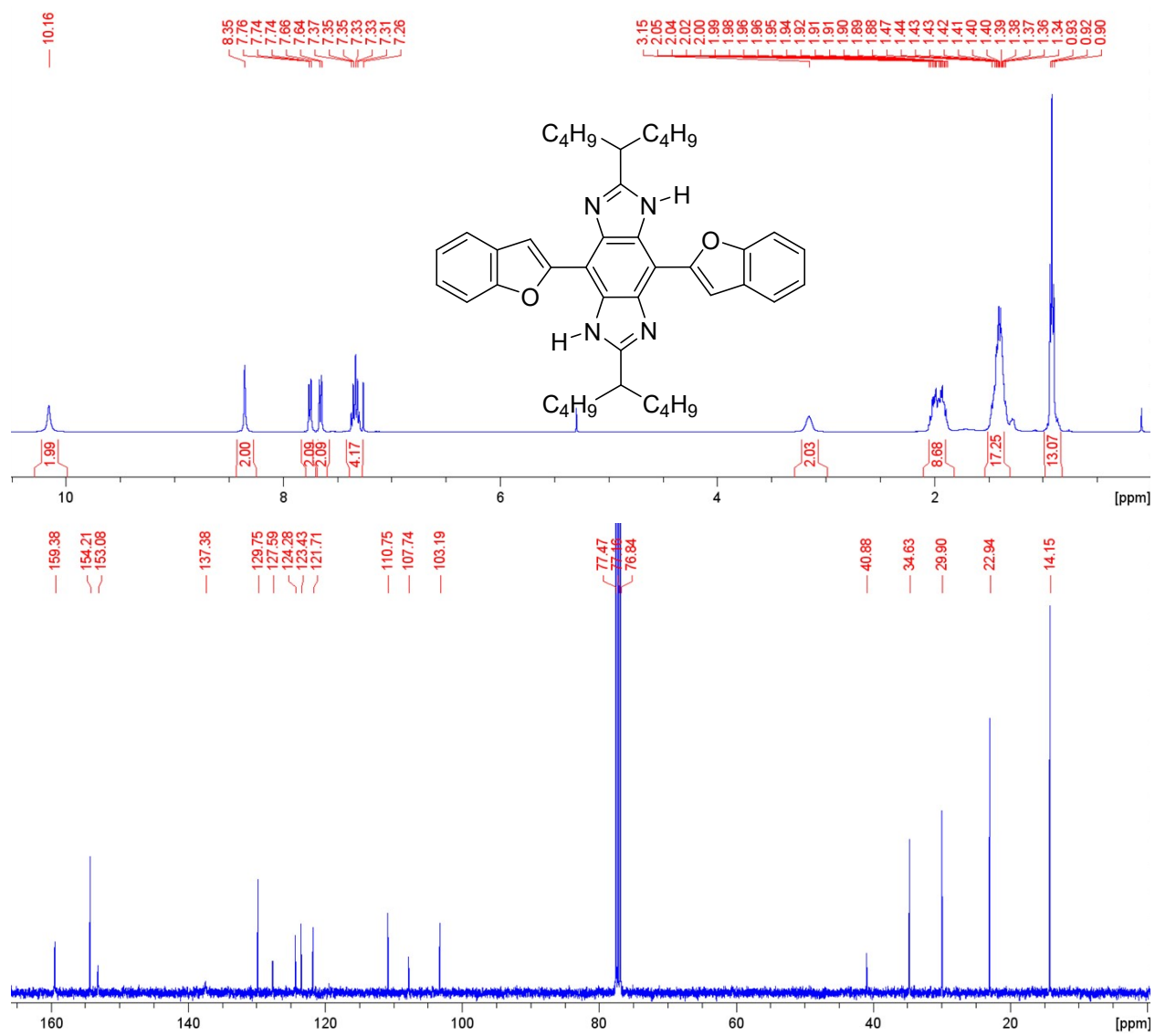


Figure S8. ¹H (400 MHz) and ¹³C{¹H} (100 MHz) NMR spectra of **5** at room temperature in CDCl₃.

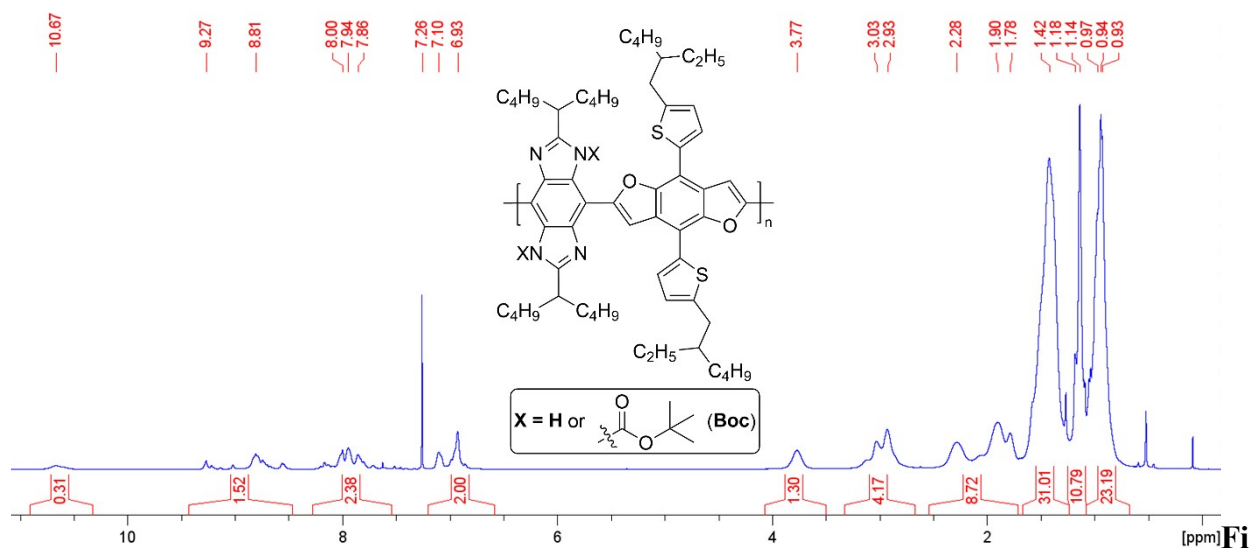


Figure S9. ^1H (400 MHz) NMR spectra of **BocP-a** ($M_n = 16.1$ kg/mol, $\bar{D} = 1.42$) at room temperature in CDCl_3 where X exists as either Boc or H due to Boc-deprotection occurring during polymerization.

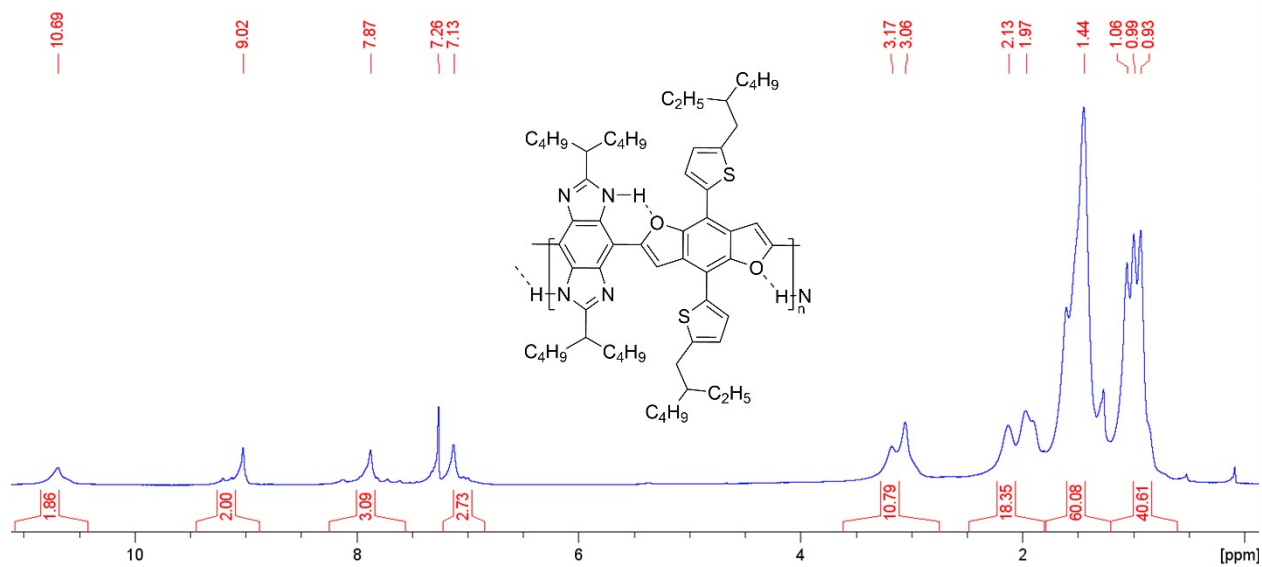


Figure S10. ^1H (400 MHz) NMR spectra of **HPLP-a** (**BocP-a**: $M_n = 16.1$ kg/mol, $\bar{D} = 1.42$) at room temperature in CDCl_3 .

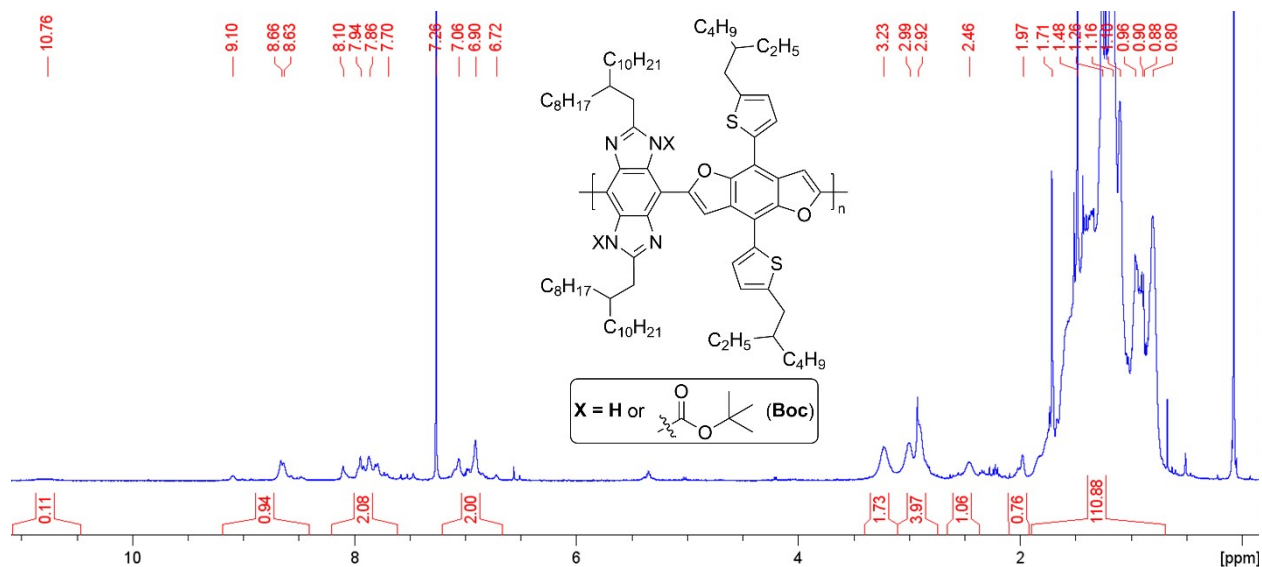


Figure S11. 1H (400 MHz) NMR spectra of **BocP-b** ($M_n = 13.5$ kg/mol, $\bar{D} = 1.30$) at room temperature in $CDCl_3$ where X exists as either Boc or H due to Boc-deprotection occurring during polymerization.

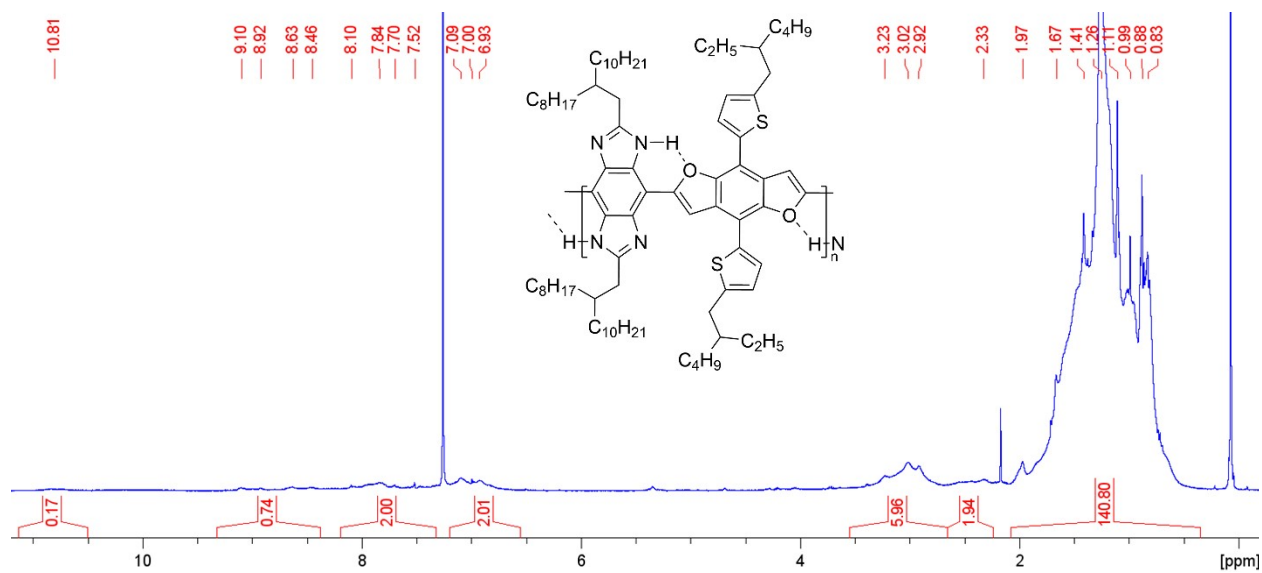


Figure S12. 1H (400 MHz) NMR spectra of **HPLP-a** (**BocP-b**: $M_n = 13.5$ kg/mol, $\bar{D} = 1.30$) at room temperature in $CDCl_3$.

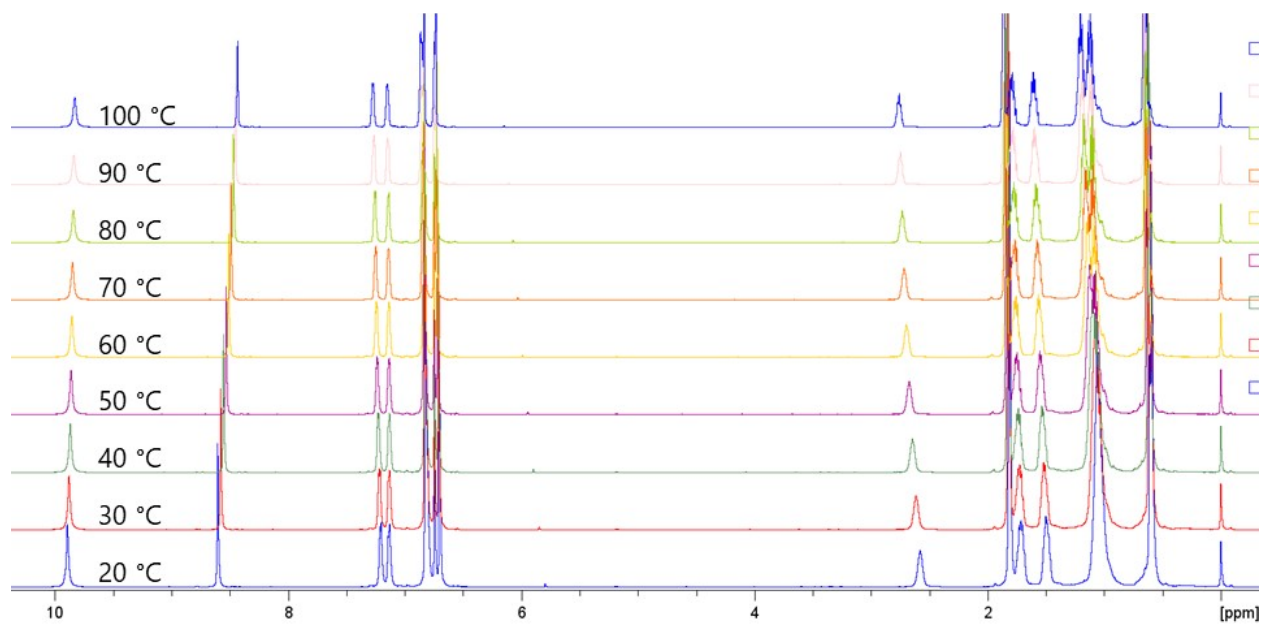


Figure S13. Variable-temperature ^1H (500 MHz) NMR spectra of **5** in $\text{C}_6\text{D}_5\text{CD}_3$.

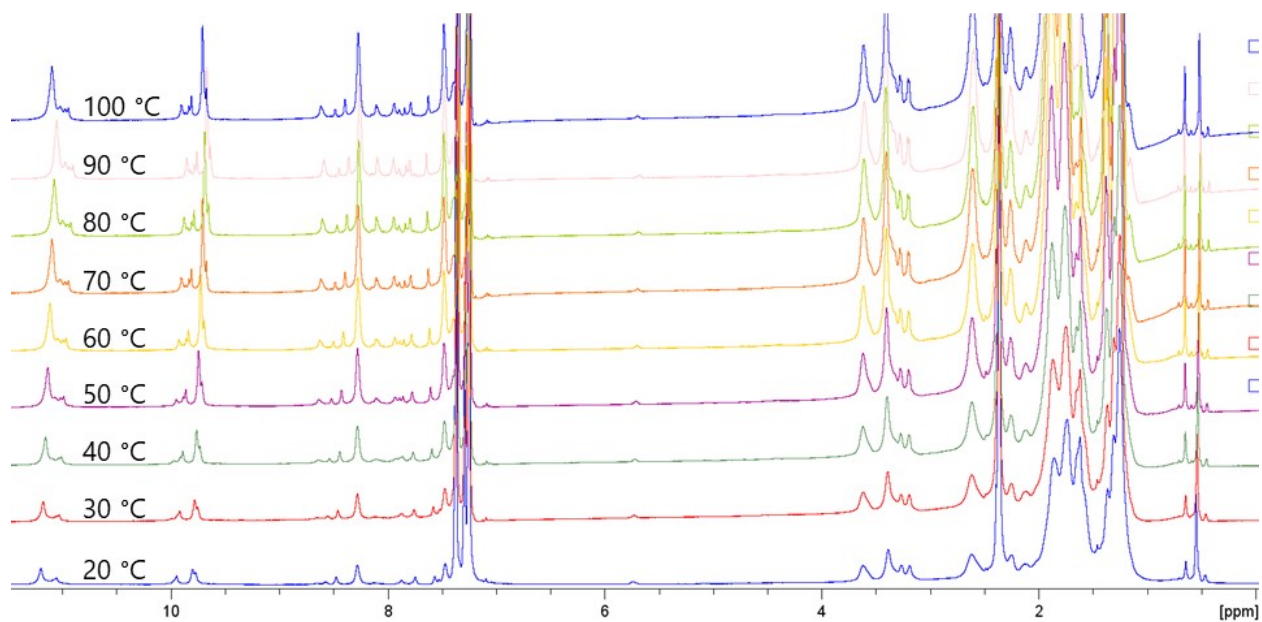


Figure S14. Variable-temperature ^1H (500 MHz) NMR spectra of **HPLP-a** (**BocP-a**: $M_n = 7.3$ kg/mol, $\bar{D} = 1.83$) in $\text{C}_6\text{D}_5\text{CD}_3$.

4. Fourier Transform Infrared Spectroscopy

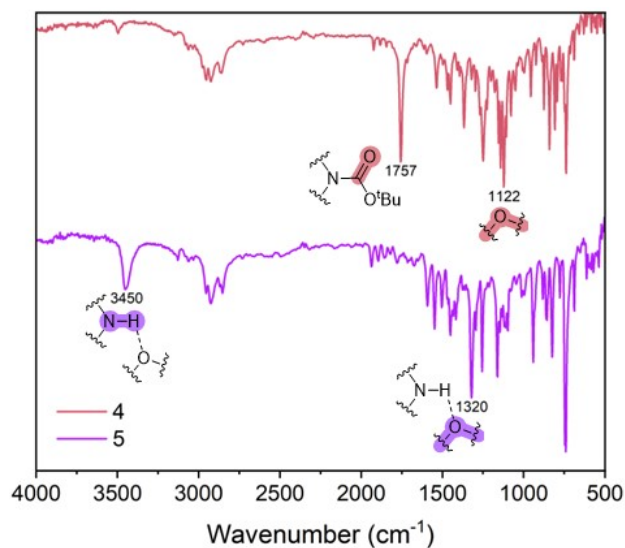


Figure S15. Fourier transform infrared spectra of small molecules **4** and **5** in the solid state at room temperature.

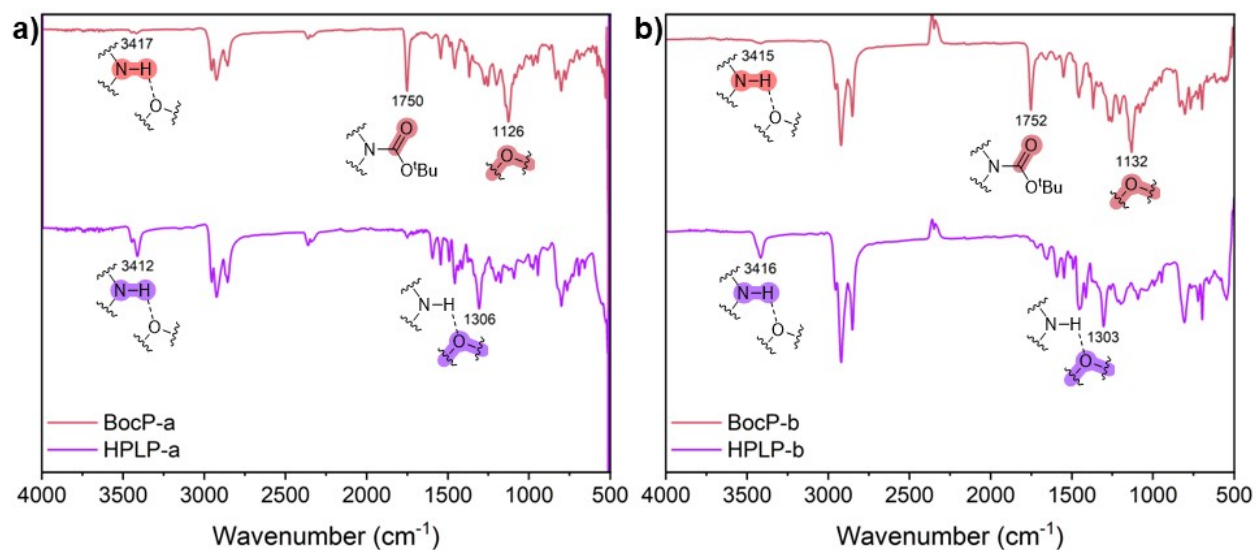


Figure S16. Fourier transform infrared spectra of polymers (a) **BocP-a** ($M_n = 11.5$ kg/mol, $\bar{D} = 2.15$) and **HPLP-a**, and (b) **BocP-b** ($M_n = 43.6$ kg/mol, $\bar{D} = 1.76$) and **HPLP-b** in the solid state at room temperature.

5. Gel Permeation Chromatography

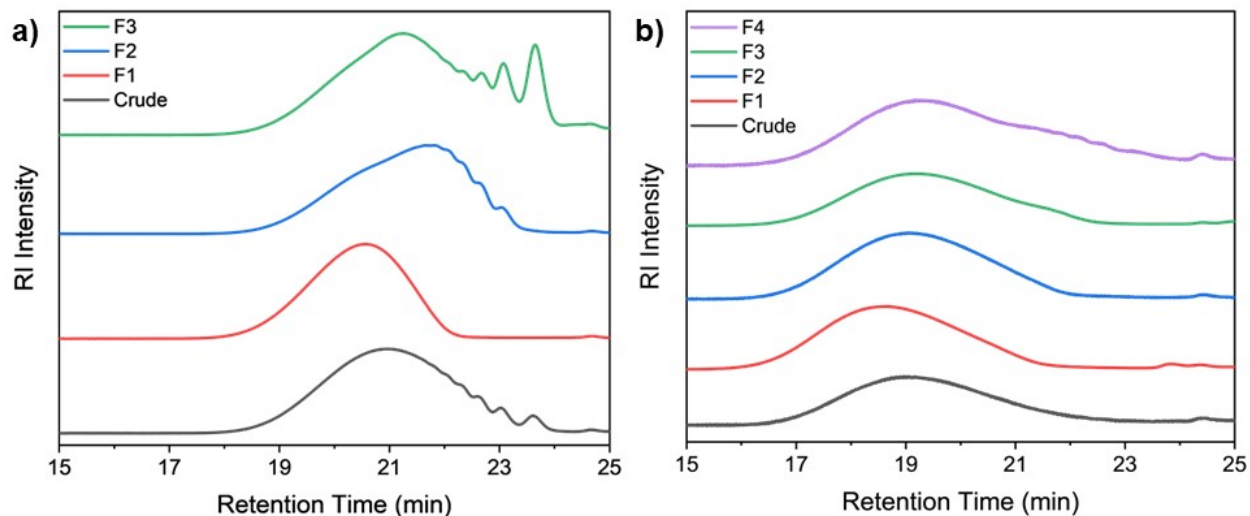


Figure S17. Analytical gel permeation chromatography (GPC) of crude polymers and the fractions purified and collected via preparative GPC of (a) **BocP-a** and (b) **BocP-b**.

Table S1. Molar mass data for **BocP-a** and **BocP-b**. ^aSample isolated for NMR analysis and cyclic voltammetry measurements ^bSample isolated for scanning tunneling microscopy

Polymer	Fraction	% Yield	M_w (kg/mol)	M_n (kg/mol)	\bar{D}
BocP-a	Crude	-	24.7	11.5	2.15
	1	21%	22.9	16.1	1.42
	2	48%	13.4	7.3	1.83
	3	23%	12.0	4.1	2.94
BocP-b	Crude	-	56.6	28.6	1.98
	1	26%	76.9	43.6	1.76
	2	16%	58.4	32.4	1.80
	3	18%	52.2	26.5	1.97
	4	23%	43.6	14.3	3.19
BocP-b^a	-	-	17.5	13.5	1.30
BocP-b^b	-	-	19.3	12.8	1.50

6. Thermal Properties

Thermogravimetric analysis (TGA) experiments were carried under nitrogen flow at a heating rate of $20\text{ }^{\circ}\text{C min}^{-1}$ from $\sim 20\text{ }^{\circ}\text{C}$ to $800\text{ }^{\circ}\text{C}$ using a Perkin Elmer TGA-7. Differential Scanning Calorimetry (DSC) experiments were carried out under nitrogen flow with a heating/cooling rate of $5\text{ }^{\circ}\text{C min}^{-1}$ beginning from $\sim 40\text{ }^{\circ}\text{C}$ and covering a range between -30 to $280\text{ }^{\circ}\text{C}$ for an initial cycle followed by a second melt from 40 to $280\text{ }^{\circ}\text{C}$ using a Dupont 2100 Calorimeter.

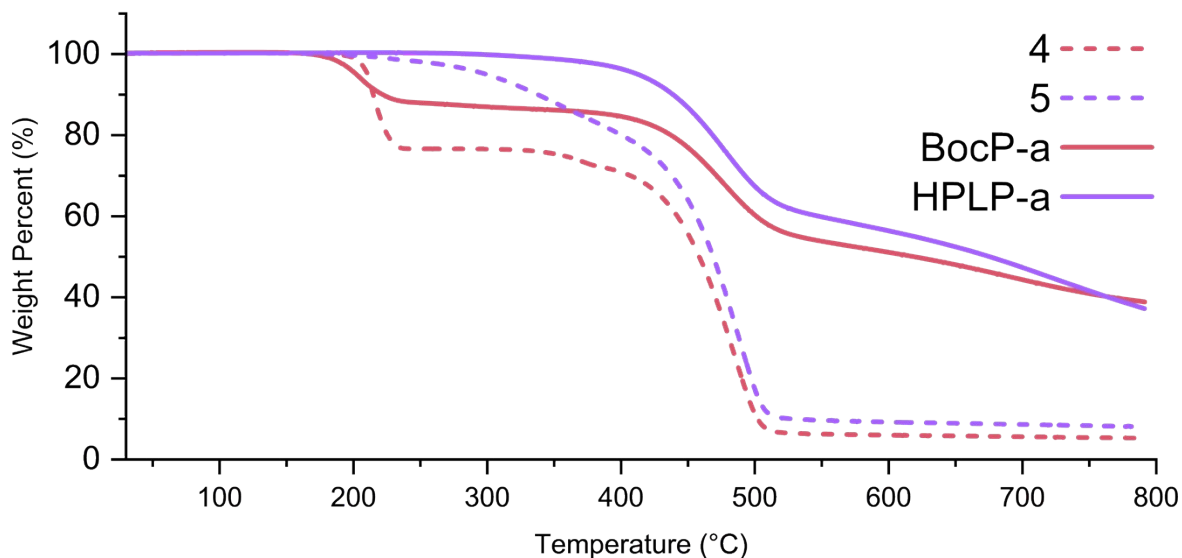


Figure S18. Thermogravimetric Analysis of small molecules **4** and **5** and polymers **BocP-a** ($M_n=16.1\text{ kg/mol}$, $\bar{D}=1.42$) and **HPLP-a**.

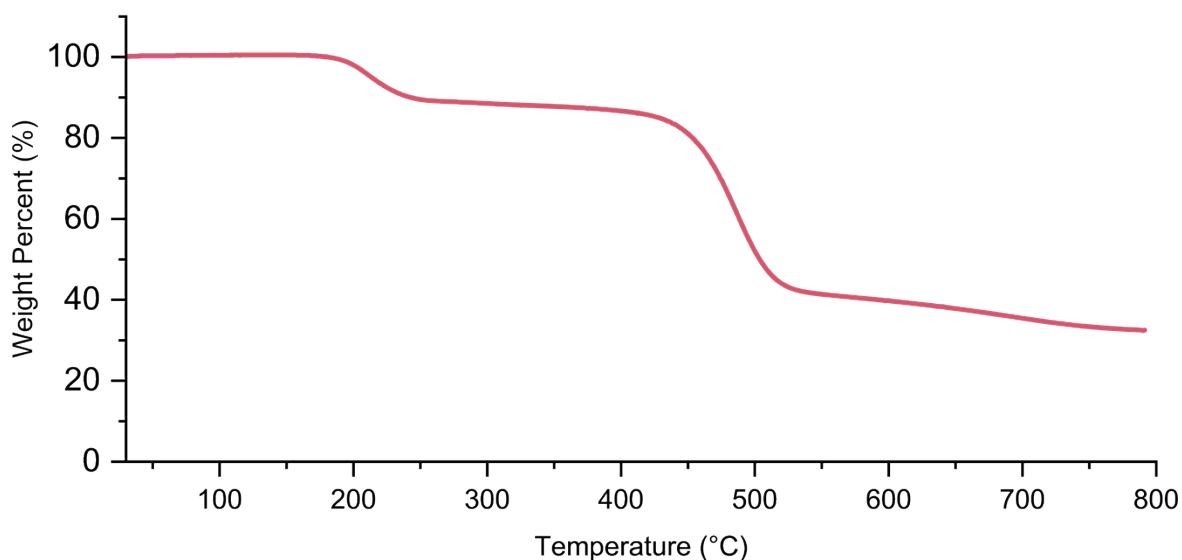


Figure S19. Thermogravimetric Analysis of **BocP-b** ($M_n=28.6\text{ kg/mol}$, $\bar{D}=1.98$).

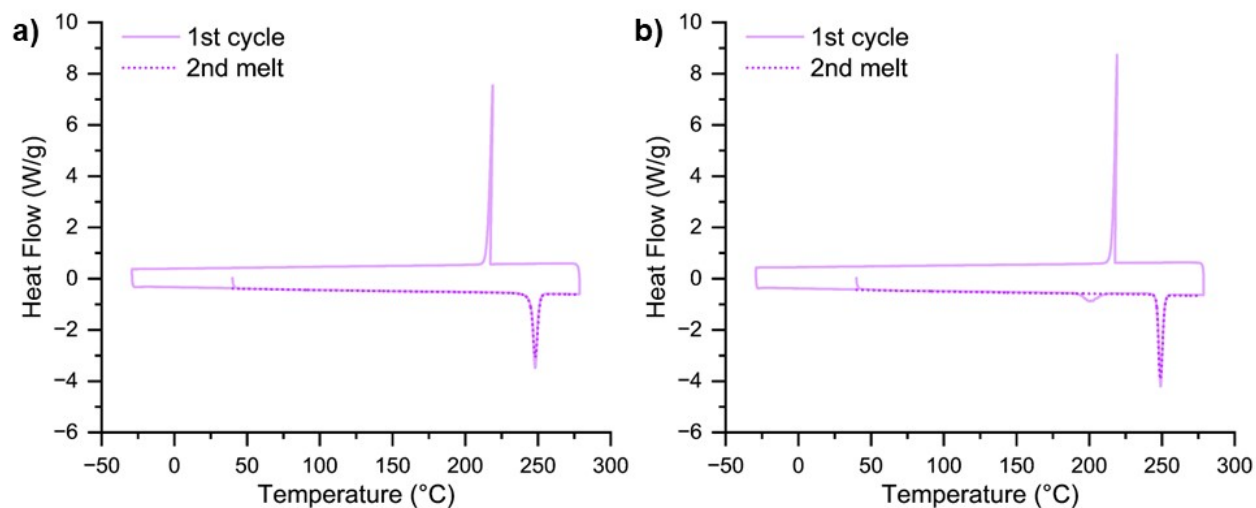


Figure S20. Differential scanning calorimetry of (a) powder and (b) single crystal samples of molecule 5.

7. Solvent Resistance

Qualitative solubility and solvent resistance experiments were conducted with samples of **BocP-a** ($M_n = 16.1$ kg/mol, $D = 1.42$) and **BocP-b** ($M_n = 43.6$ kg/mol, $D = 1.76$) and their respective H-bonded forms. There are four different terms used to qualitatively describe solubility which are:

Soluble – Sample easily dissolved in concentrations > 5 mg/mL.

Slightly Soluble – Thin film is partially dissolved, and polymer color is observed in solution.

Scarcely Soluble – Thin film not visibly dissolved, but polymer can be detected in solution via fluorescence spectroscopy.

Insoluble – Polymer cannot be detected in solution via fluorescence spectroscopy.

To test solvent resistance of **HPLP** films, **BocP** was drop-casted onto glass substrates and annealed at 180 °C for 1 hour to convert to their H-bonded forms. Films were submerged in ~ 5 mL of solvent for 1 hour before recording physical observations of solution or analyzing using fluorescence spectroscopy.

Table S2. Solubility of **BocP-a** and **BocP-b** in various organic solvents.

Sample	Solubility in:					
	Hexane	Toluene	Chlorobenzene	Chloroform	Tetrahydrofuran	Ethyl Acetate
BocP-a	<0.1 mg/mL	Soluble	Soluble	Soluble	Soluble	<0.5 mg/mL
BocP-b	~1.7 mg/mL	Soluble	Soluble	Soluble	Soluble	~3.5 mg/mL
HPLP-a	Scarcely Soluble	Slightly Soluble	Slightly Soluble	Slightly Soluble	Slightly Soluble	Scarcely Soluble
HPLP-b	Insoluble	Scarcely Soluble	Scarcely Soluble	Scarcely Soluble	Scarcely Soluble	Insoluble

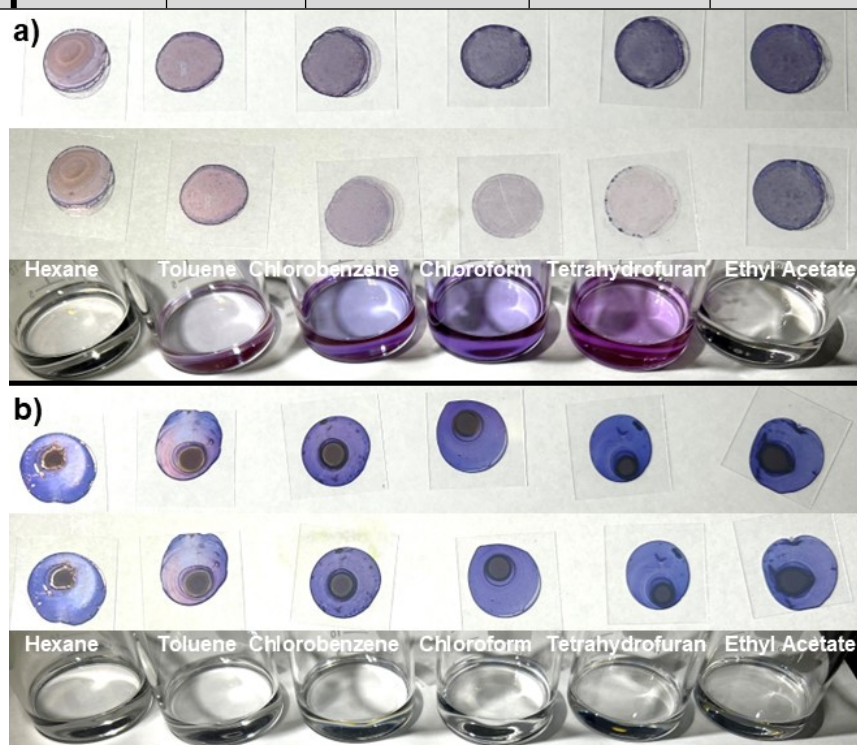


Figure S21. Images of (a) **HPLP-a** and (b) **HPLP-b** thin films before (top) and after (middle) soaking in various organic solvents for 1 hour, and the appearance of their respective solutions after soaking.

8. UV-Vis and Fluorescence Spectroscopy

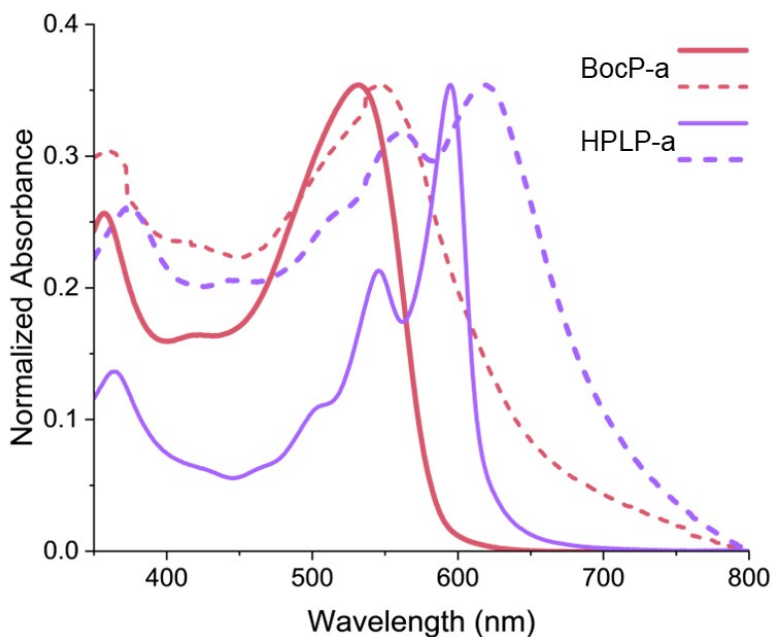


Figure S22. Normalized UV-Vis absorption spectra of solution-phase (solid line) and thin film (dashed line) samples of **BocP-a** ($M_n = 16.1$ kg/mol, $D = 1.42$) and **HPLP-a**. Solutions were prepared at a concentration of 10^{-5} M in CHCl_3 . Solid-phase thin films were formed by drop-casting CH_2Cl_2 solutions (10^{-3} M) of polymer samples.

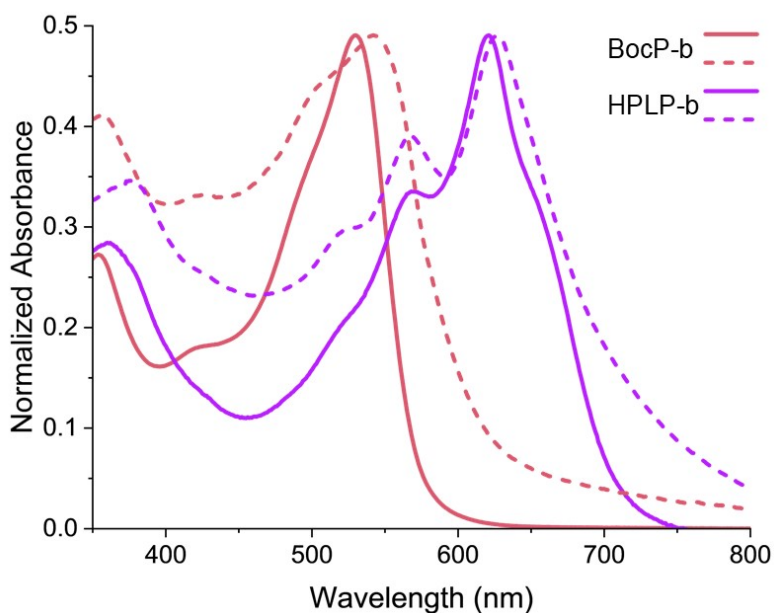


Figure S23. Normalized UV-Vis absorption spectra of solution-phase (solid line) and thin film (dashed line) samples of **BocP-b** ($M_n = 43.6$ kg/mol, $\bar{D} = 1.76$) and **HPLP-b**. Solutions were prepared at a concentration of 10^{-5} M in CHCl_3 . Solid-state thin films were formed by drop-casting CH_2Cl_2 solutions (10^{-3} M) of polymer samples.

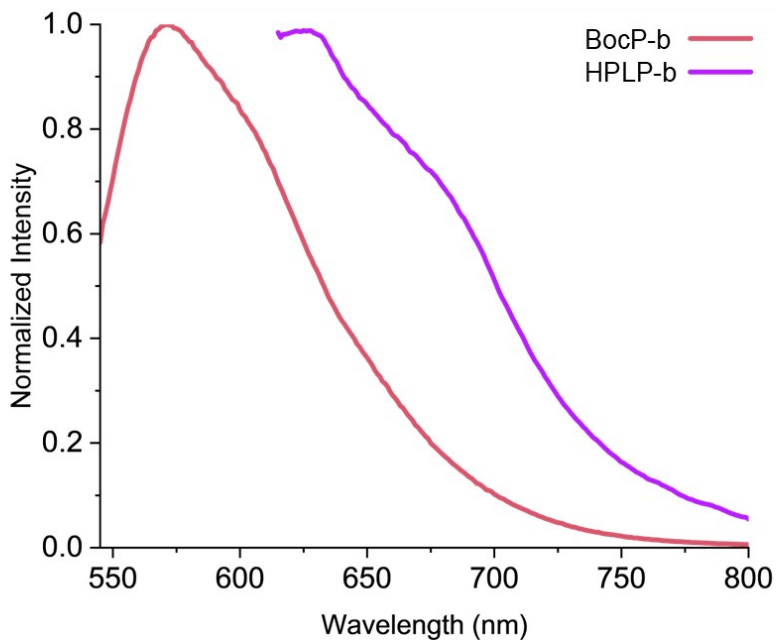


Figure S24. Normalized fluorescence emission spectra of **BocP-b** ($M_n = 43.6$ kg/mol, $\bar{D} = 1.76$) and **HPLP-b**. Solutions were prepared at a concentration of 10^{-7} M in CHCl_3 .

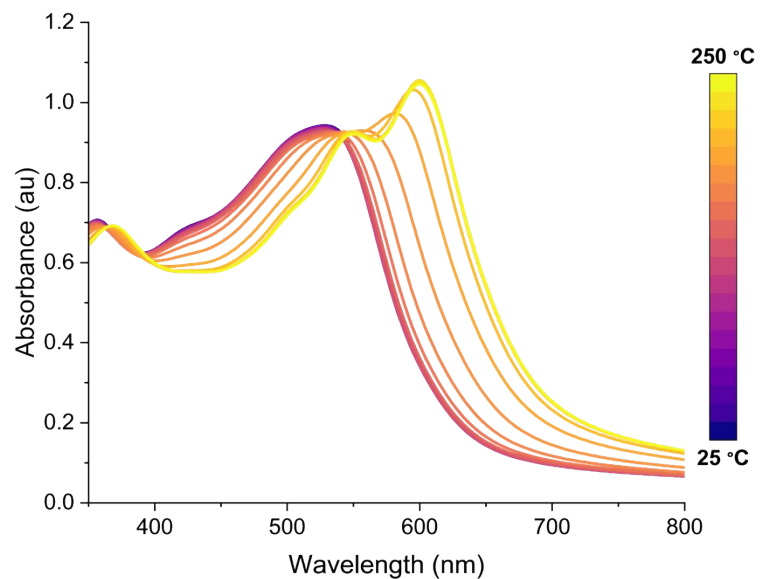


Figure S25. Solid-state variable-temperature UV-Vis absorption spectra of **BocP-a** ($M_n = 16.1$ kg/mol, $D = 1.42$) thin film showing conversion to **HPLP-a** while heating from 25 to 250 °C.

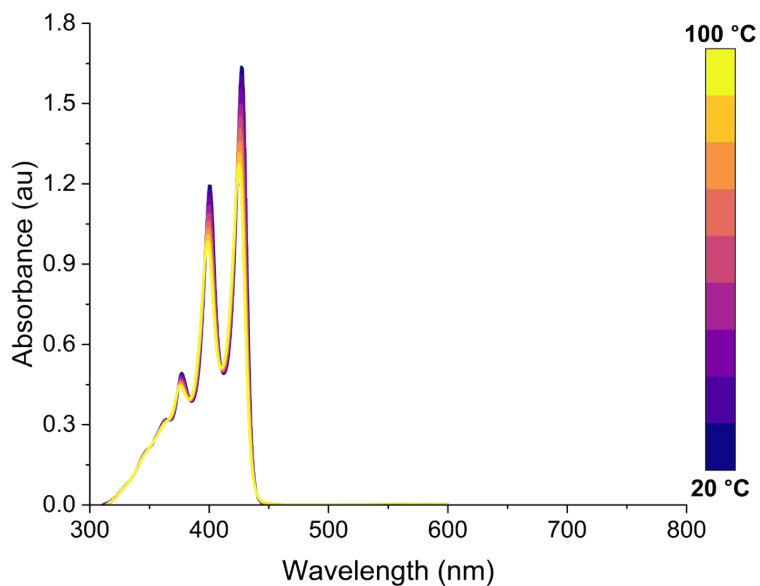


Figure S26. Variable-temperature UV-Vis absorption spectra of **5** while heating from 20 to 100 °C at a concentration of 1.56×10^{-5} M in toluene.

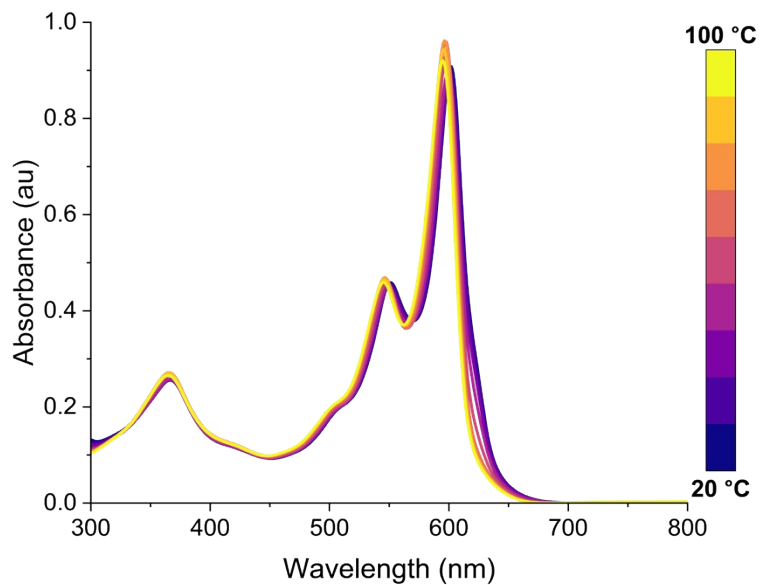


Figure S27. Variable-temperature UV-Vis absorption spectra of **HPLP-a (BocP-a: $M_n = 16.1$ kg/mol, $\bar{D} = 1.42$)** while heating from 20 to 100 °C at a concentration of 10^{-5} M in toluene.

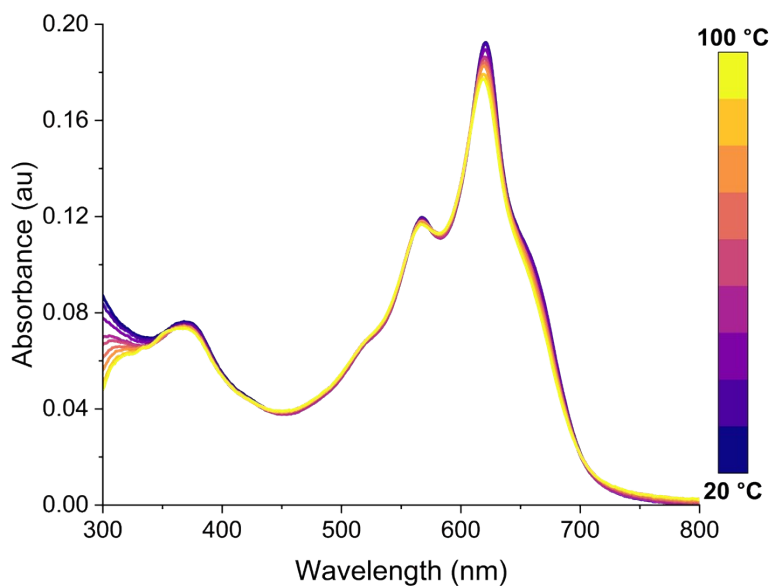


Figure S28. Variable-temperature UV-Vis absorption spectra of **HPLP-b (BocP-b: $M_n = 43.6$ kg/mol, $\bar{D} = 1.76$)** in toluene while heating from 20 to 100 °C at a concentration of 10^{-5} M in toluene.

9. Cyclic Voltammetry

Cyclic voltammetry (CV) experiments were carried out in nitrogen-purged CH₂Cl₂ at room temperature with a CHI voltametric analyzer. Tetra-n-butylammonium hexafluorophosphate (0.1 mol/L) was used as the supporting electrolyte. The conventional three-electrode configuration consisted of a platinum working electrode, a platinum wire auxiliary electrode, and an Ag/AgCl electrode with ferrocene/ferrocenium as the standard. Cyclic voltammograms were obtained at a scan rate of 100 mV/s.

The energy levels were calculated using ferrocene/ferrocenium (Fc/Fc⁺) as the standard reference.

Fc/Fc⁺ vs Ag/AgCl = 0.45 V.

$E_{\text{HOMO/LUMO}} = -4.80 + (E_{1/2}) \text{ eV}$

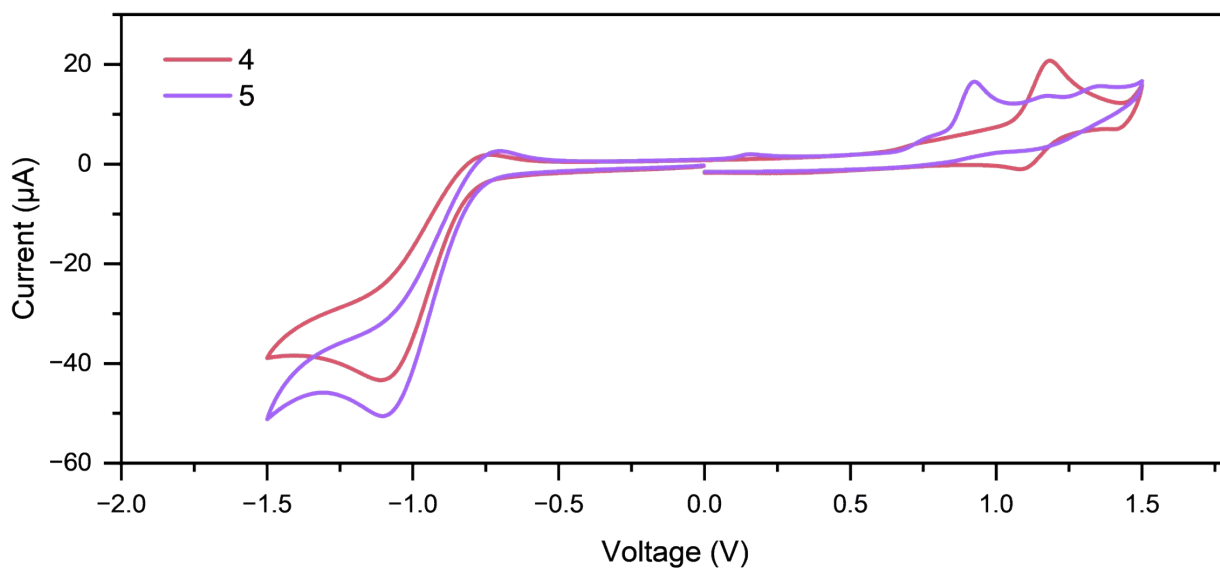


Figure S29. Cyclic voltammograms of molecules **4** and **5** measured in 0.1 M tetrabutyl ammonium hexafluorophosphate dichloromethane solutions vs Fc/Fc⁺.

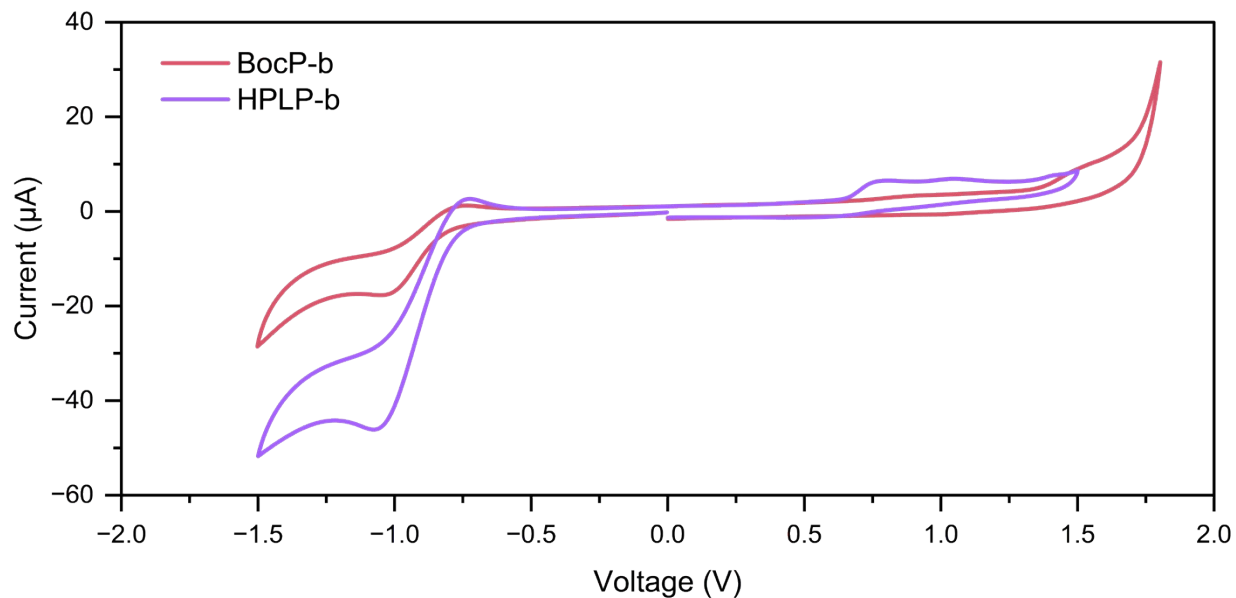
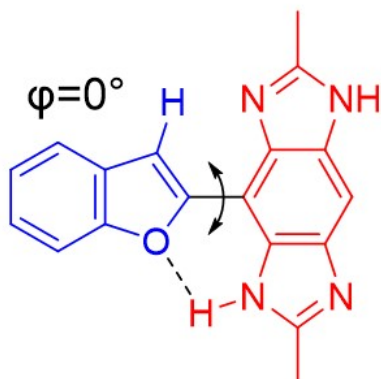


Figure S30. Cyclic voltammograms of molecules **BocP-b** ($M_n = 13.5$ kg/mol, $\mathcal{D} = 1.30$) and **HPLP-b** polymers in 0.1 M tetrabutyl ammonium hexafluorophosphate dichloromethane solutions vs Fc/Fc^+ .

10. Density Functional Theory Computation



Rotational barrier
 = 9.62 kcal/mol
 $\langle \cos^2(\varphi) \rangle = 0.925$

Figure S31. Model benzobisimidazole-benzofuran system used for torsional analysis at B3LYP/6-31G(d) level of theory.

Table S3. Atom coordinates and total energy of optimized benzobisimidazole-benzofuran ($\varphi = 0^\circ$) system shown in Figure S28.

Total Energy: -988.384179 Hartrees. Zero Imaginary Frequencies.

Atom	X	Y	Z
C	1.09843400	-1.25322500	-0.00002700
C	2.49046400	-1.56590800	0.00005900
C	2.95232200	0.73739000	0.00005600
C	1.56548500	1.06086700	-0.00002500
N	2.67236000	-2.94236000	0.00007700
N	1.39661100	2.43789100	-0.00009500
C	1.46307300	-3.45291700	0.00001800
C	2.60843000	2.94548600	-0.00005100
C	1.14410100	-4.91229100	-0.00004300
H	2.07815200	-5.47674700	0.00031200
H	0.56172900	-5.19747800	0.88506300
H	0.56236100	-5.19751800	-0.88554400
C	2.93250500	4.40345900	-0.00002900
H	3.51403600	4.68830700	0.88583800
H	3.51495300	4.68816100	-0.88533400
H	2.00028900	4.97087400	-0.00054200
N	3.58441100	1.97433300	0.00017400
H	4.58105000	2.13193400	-0.00024300
N	0.47734700	-2.48927300	-0.00010700
H	-0.52302800	-2.62212100	0.00028100
C	0.57567900	0.05060700	-0.00006400
C	-0.84056800	0.34747200	-0.00006700
O	-1.70207600	-0.75090400	-0.00005100
C	-1.55019800	1.51590700	-0.00003900
C	-2.97741300	-0.24860300	-0.00006900
C	-2.94196800	1.15943200	-0.00007500
H	-1.10337500	2.49829900	-0.00011500
C	3.45840100	-0.55830200	0.00008900
H	4.51786800	-0.79213500	0.00017100
C	-4.15908000	1.86030300	0.00005800
H	-4.17268100	2.94657900	0.00008200
C	-5.34650500	1.13333900	0.00011500
H	-6.29643500	1.66085600	0.00021700
C	-5.34418200	-0.27371900	0.00007300
H	-6.28833200	-0.81084500	0.00011100
C	-4.14807200	-0.99363900	-0.00001400
H	-4.13053600	-2.07901800	-0.00002400

D 4 21 22 24 F

11. Scanning Tunneling Microscopy

Scanning tunneling microscopy (STM) images were acquired in ultrahigh vacuum (UHV) using a variable-temperature STM (VT-STM) equipped with a 4-stage Molecularspray electro spray deposition (ESD) system. The VT-STM (SPECS STM 150 Aarhus) was cooled with liquid nitrogen, reaching temperatures around $-145\text{ }^{\circ}\text{C}$ during the measurements. Polymers were deposited by ESD from solution into the UHV chamber on room temperature Au(111)/mica (Georg Albert PVD, 300 nm thickness). The solutions were prepared by dissolving the polymers in chloroform at a concentration of approximately 0.025 g/L, with methanol added in a 4:1 volume ratio. The deposition current was monitored on the target substrate with a Keithley 617 Programmable Electrometer, resulting in a deposition charge of about 10 pAh. Prior to deposition, atomically flat and clean Au(111)/mica substrates were prepared in UHV by cycles of argon sputtering (1 kV) and annealing at $500\text{ }^{\circ}\text{C}$. All images were acquired in constant current feedback mode using an electrochemically etched tungsten tip, which was cleaned by argon sputtering after insertion into UHV to remove any oxide layer. The STM images were processed with WSxM and Gwyddion, while molecular models were created and optimized in Avogadro.^{S3-S5} The superposition of the models onto STM images was performed using the LMAPper software.^{S6}

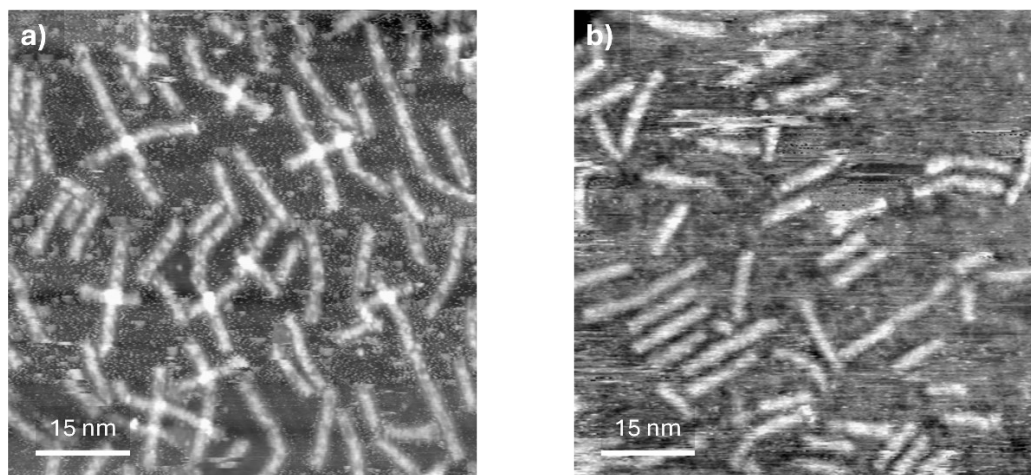


Figure S32. STM images of low coverage areas of (a) **BocP-b** and (b) **HPLP-b**. Both polymers appear to possess overall rigid, linear backbones.

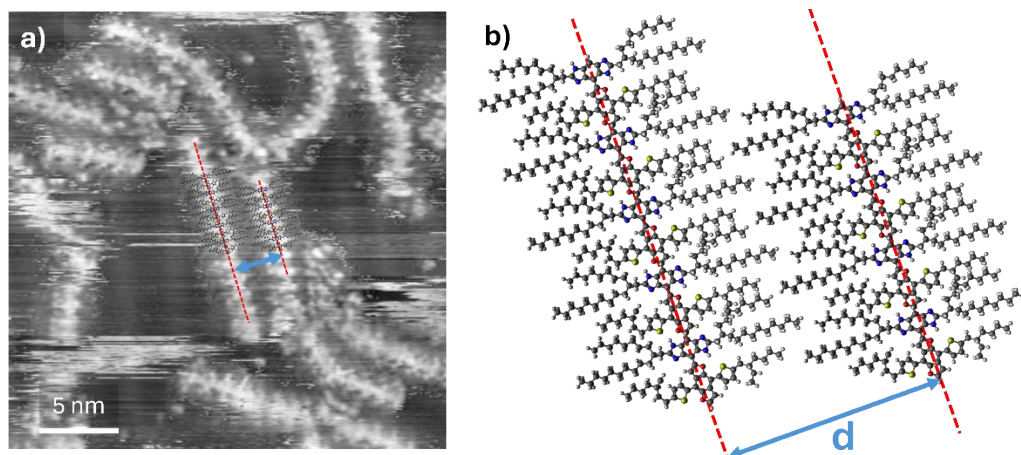


Figure S33. (a) High-resolution STM image of **HPLP-b** showing locally straight and parallel polymer strands with a molecular model of the polymer structure superposed in the center. The average distance between parallel polymer strands, determined by analyzing around 100 adjacent polymers across various STM images, is $d = 3.4 \pm 0.5$ nm. This value is consistent with a distance $d = 3.5$ nm calculated for the 2D model shown in (b) where the side chains exhibit minimal interlocking between their branched arms. In the model, d is estimated by assuming fully extended side chains, with the separation at their ends corresponding to twice the van der Waals radius of hydrogen.

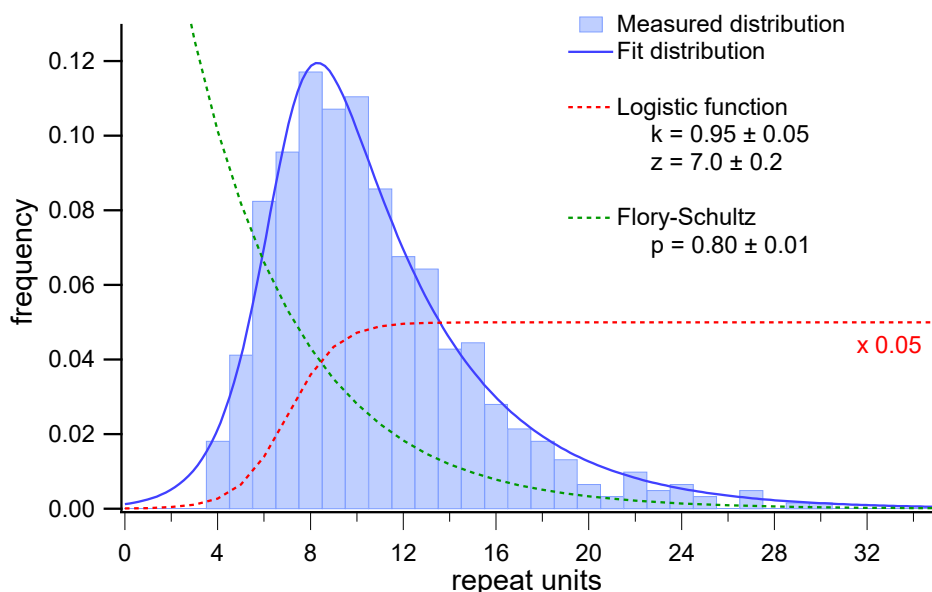


Figure S34. Mass distribution curve of **BocP-b** obtained from the ESD-STM analysis.

A total of 607 polymer chains were identified across different STM images and their length profiles were used to build the histogram in Figure S31. The data were fitted using the product of a Flory-Schulz geometric distribution—which models the polymer growth process—and a logistic function—which accounts for the Soxhlet extraction process used to filter out shorter oligomers, unreacted monomers and residual catalysts.^{S7} The overall function, describing the probability of finding a polymer of length x is given by:

$$\text{Pr}(x) = C \frac{1}{1 + e^{-k(x-x_0)}} p^{x-1} (1-p)$$

where C is a normalizing constant, k is the steepness of the logistic curve, x_0 is its centre and p is the extent of reaction in the Flory–Schulz distribution. From the full mass distribution, we determined $M_n = 15.6$ kg/mol, $M_w = 18.2$ kg/mol and $D_n = 1.17$. Although these values appear to be in agreement with those obtained by GPC, the full mass distributions derived from the two techniques differ significantly. The mass distributions of conjugated polymers obtained from GPC are known to be influenced by several factors, including calibration based on polystyrene standards, polymer aggregation leading to mass overestimation and the inherent uncertainty associated with molecular mass values due to the subjective nature of baseline signal subtraction. Consequently, the results obtained from ESD-STM analysis should be regarded as a more accurate determination of the polymer mass distribution.^{S7}

12. Field-Effect Transistor Device Fabrication and Measurement

Treatment of Substrates. Heavily doped n-type Si wafers with 300 nm SiO₂ were used as substrates for thin film organic field effect transistors (OFET). The wafers were prepared according to literature procedure^{S8} via cleaning with piranha solution (H₂SO₄:H₂O₂ = 7:3), oxidization under ozone treatment, and spin-coating with a solution of n-octadecyltrichlorosilane (OTS) in toluene.

Fabrication and Measurement of Organic Field Effect Transistors. Organic field effect transistors were fabricated by spin-coating the organic polymer **BocP** at a concentration of 5 mg/mL on OTS-modified SiO₂/Si with a bottom-gate/top-contact architecture. Spin-coating was done at 1000 RPM for 60 seconds. Then 50 nm Au as source and drain electrodes were deposited on the film by physical vapor deposition and templated by shadow masks with defined channel

lengths of 125 μm and widths of 3 mm. The OFET characteristics were recorded using Lakeshore CPX-HF Probe Station under nitrogen atmosphere. The mobility was calculated by the formula: $I_D = W/2L\mu C_i (V_G - V_T)^2$ where I_D is the drain-source current, and are the channel width and length, C_i is the dielectric capacitance, V_G is the gate voltage, and V_T is the threshold voltage.

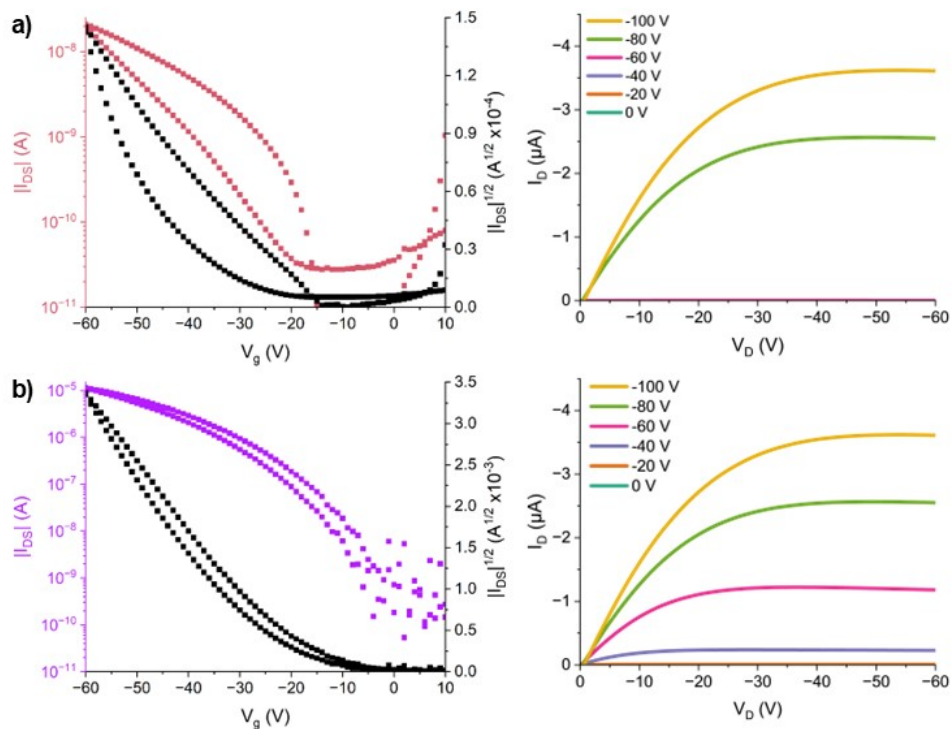


Figure S35. Transfer curves at $V_{DS} = 60$ V (left) and output (right) curves of (a) **BocP-a** ($M_n = 16.1$ kg/mol, $\bar{D} = 1.42$; $\mu_h = 5.2 \times 10^{-5}$ $\text{cm}^2 \text{V}^{-1} \text{s}^{-1}$) and (b) **HPLP-a** ($\mu_h = 4.6 \times 10^{-2}$ $\text{cm}^2 \text{V}^{-1} \text{s}^{-1}$).

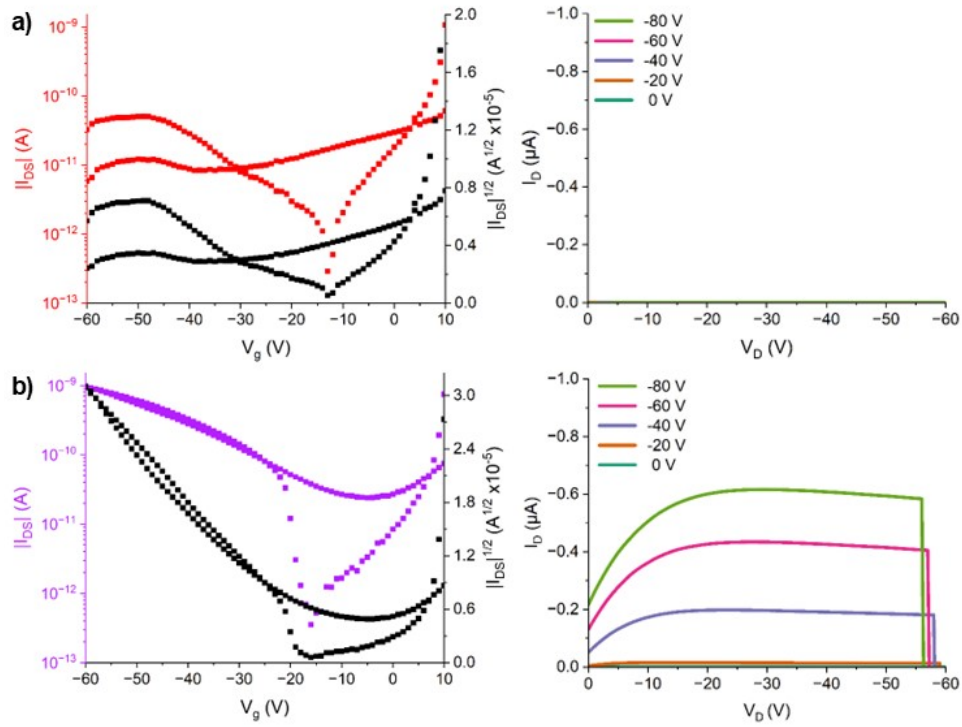


Figure S36. Transfer curves at $V_{DS} = 60$ V (left) and output (right) curves of (a) **BocP-b** ($M_n = 43.6$ kg/mol, $\bar{D} = 1.76$; $\mu_h = 8.5 \times 10^{-9} \text{cm}^2 \text{V}^{-1} \text{s}^{-1}$) and (b) **HPLP-b** ($\mu_h = 3.4 \times 10^{-6} \text{cm}^2 \text{V}^{-1} \text{s}^{-1}$).

13. Atomic Force Microscopy

Atomic force microscopy (AFM) images were recorded with a Bruker Dimension Icon AFM in a tapping mode and processed using NanoScope Analysis.

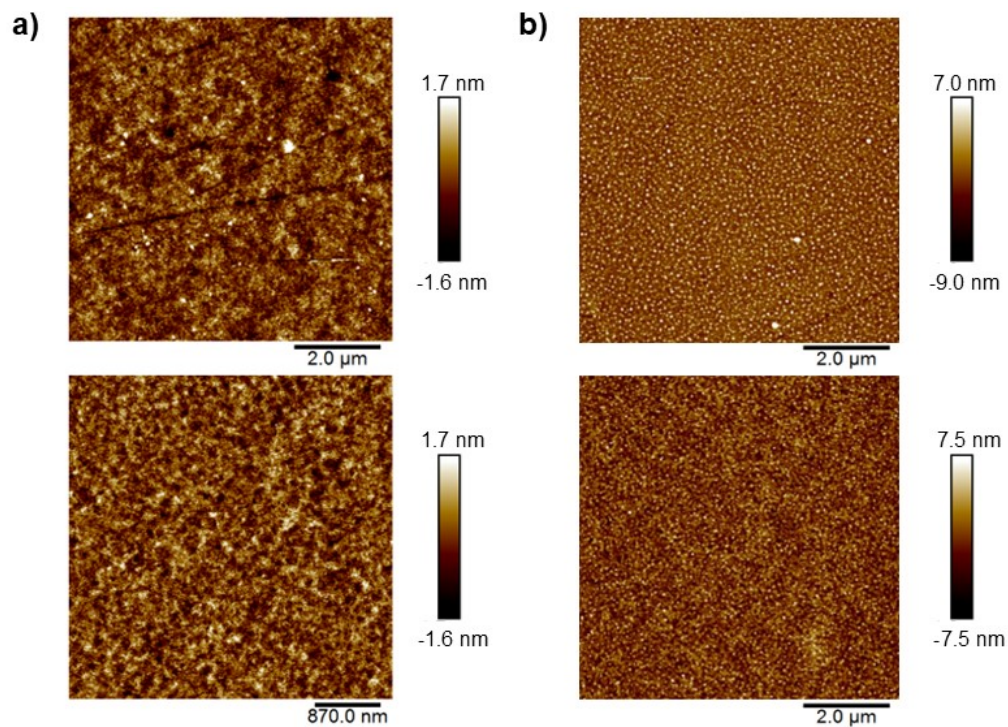


Figure S37. AFM images of the films used for OFET device: (a) **BocP-a** (top) and **HPLP-a** (bottom) and (b) **BocP-b** (top) and **HPLP-b** (bottom).

14. References

- [S1] Le, H. T. M.; El-Hamdi, N. S.; Miljanić, O. S. Benzobisimidazole Cruciform Fluorophores. *The Journal of Organic Chemistry* **2015**, *80*, 5210-5217.
- [S2] Zhang, Z.; Zhang, B.; Han, X.; Chen, H.; Xue, C.; Peng, M.; Ma, G.; Ren, Y. Stille type P–C coupling polycondensation towards phosphorus-crosslinked polythiophenes with P-regulated photocatalytic hydrogen evolution. *Chemical Science* **2023**, *14*, 2990-2998.
- [S3] Horcas, I.; Fernández, R.; Gómez-Rodríguez, J. M.; Colchero, J.; Gómez-Herrero, J.; Baro, A. M. WSXM: A software for scanning probe microscopy and a tool for nanotechnology. *Review of Scientific Instruments* **2007**, *78*, 013705-013713.
- [S4] Nečas, D.; Klapetek, P. Gwyddion: An open-source software for SPM data analysis. *Central European Journal of Physics* **2012**, *10*, 181-188.
- [S5] Hanwell, M. D.; Curtis, D.E.; Lonie, D.C.; Vandermeersch, T.; Zurek, E.; Hutchison, G. R. Avogadro: An advanced semantic chemical editor, visualization, and analysis platform. *Journal of Cheminformatics* **2012**, *4*, 1-17.
- [S6] LMAPper - The SPM and Mol Viewer | Reviews SourceForge.net. <https://sourceforge.net/projects/spm-and-mol-viewer/reviews>.
- [S7] Moro, S.; Spencer, S. E. F.; Lester, D. W.; Nubling, F.; Sommer, M.; Costantini, G., Molecular-Scale Imaging Enables Direct Visualization of Molecular Defects and Chain Structure of Conjugated Polymers. *ACS Nano* **2024**, *18*, 11655-11664.
- [S8] Ito, Y.; Virkar, A. A.; Mannsfeld, S.; Oh, J. H.; Toney, M.; Locklin, J.; Bao, Z. Crystalline Ultrasmooth Self-Assembled Monolayers of Alkylsilanes for Organic Field-Effect Transistors. *Journal of the American Chemical Society* **2009**, *131*, 9396-9404.